Hindawi
Geofluids
Volume 2023, Article ID 6459544, 21 pages
https://doi.org/10.1155/2023/6459544

Research Article

Secondary Migration Trend Based on Basin Modeling: A Case Study of the Cambrian Petroleum System in the Tarim Basin

Yong Yue,[1] Bin Li,[2,3] Peng Wei,[2] Xin Zhang,[2] Kun Zhang,[2] Yang Suju,[4] and Xu Qingqi[4]

[1]*Wuhan Geological Survey Center, China Geological Survey, 430205 Wuhan, China*
[2]*School of Geoscience and Technology, Southwest Petroleum University, 610500 Chengdu, China*
[3]*Natural Gas Geology Key Laboratory of Sichuan Province, Southwest Petroleum University, 610500 Chengdu, China*
[4]*Design and Planning Institute of SINOPEC Northwest Company, Urumqi 830011, China*

Correspondence should be addressed to Bin Li; libinxnsy@outlook.com

Received 6 November 2022; Revised 3 January 2023; Accepted 31 March 2023; Published 2 May 2023

Academic Editor: Hexin Huang

Secondary hydrocarbon migration is an important aspect of oil-gas accumulation research. While previous studies have relied on geological and fluid geochemical characteristics to predict migration direction, these results are often limited by the number of samples. In recent years, basin simulation has emerged as a valuable tool in hydrocarbon migration research due to its extensive algorithms and adaptable modeling capabilities. It has obvious technical advantages especially for resource evaluation in areas with a lower exploration degree and scarce data. The deep oil and gas in the Cambrian petroleum system in the Tarim Basin is a deep hydrocarbon challenging area in China. There has been no breakthrough in exploration due to the large burial depth (generally > 6000 m) and the long accumulation and transformation processes. Therefore, predicting the secondary migration of Cambrian oil and gas has become the key to solving this problem. In this study, first, the thermal evolution of the Lower Cambrian source rocks in the Tarim Basin was recovered, and the three thermal evolution models were developed. The secondary migration process of the Cambrian petroleum system was restored using the geologic model of the source rocks and paleotectonic evolution and the latest fluid potential information. By comparing the simulation results, four secondary migration models of the ultradeep oil-gas migration and accumulation were developed: multisource, multiphase, multidirectional accumulation; multisource, multiphase, single-directional accumulation; single-source, multiphase, multidirectional accumulation; and single-source, multiphase, single-directional accumulation. The fluid potential simulation results indicate that the Cambrian oil and gas have salient inheritance characteristics. The dominant migration channels in the uplift and slope are beneficial to oil-gas migration and accumulation, and the Katake uplift and the west Bachu uplift have multisource charging accumulation. The east Bachu uplift and the Tabei uplift are oil-gas accumulation zones that are beneficial to the lower petroleum system due to the continuous charging of a single petroleum system. This fluid potential simulation provides a new solution for studying the secondary migration of deep oil and gas. It provides an important reference for studying hydrocarbon accumulation in deep and ultradeep areas.

1. Introduction

The secondary migration of ultradeep oil-gas has always been an important part of research on oil-gas accumulation and is also a challenge in research on oil-gas accumulation [1, 2]. Most scholars have judged the direction of secondary oil and gas migration based on structural features, and their results are generally consistent with the exploration status, which is often affirmed in practice [3, 4]. However, the shortcoming of this method is that it can only provide the qualitative trend and cannot yield the effective path of the fluid migration and historical evolution. Some scholars have also made good progress in determining the direction of secondary oil and gas migration based on the properties of fluids [5, 6], but application of this method is limited by a lack of sufficient samples and high costs. The fluid potential has been recognized as a quantitative method for studying secondary hydrocarbon migration in petroleum geology

theory [7], but few results have been reported in the literature. The main reason for this is that calculating the fluid potential has high geological model requirements, which requires matching the hydrocarbon system elements such as the source rock, reservoir, and trap, and it is difficult to meet these requirements in actual study. The latest basin modeling technique quantifies the source rocks and the secondary oil-gas migration process through dynamic, hydromechanical, and physical means [8–11] and has attracted increasing attention in the field of oil-gas exploration [12–14], which can provide a better reference for studying ultradeep oil-gas accumulation.

With an average burial depth of >600 m, the Cambrian system in the Tarim Basin represents one of the difficult areas of ultradeep oil-gas exploration in marine facies in China [15–18]. Wells TS1, ZS1, and LT 1 revealed the wide distribution of the oil-gas resources in the ultradeep system. The large burial depth of the Cambrian system in the Tarim Basin and the long adjustment time in the late construction and transformation phases have resulted in an extremely low degree of exploration. As a result, the secondary oil-gas migration and accumulation processes of the petroleum system remain unclear [19, 20], which limits the evaluation of the ultradeep zone and exploratory deployment. Therefore, in this study, a new method combining effective source rock data with paleotectonic evolution was developed to simulate the fluid potential of the Cambrian petroleum system, and the secondary hydrocarbon migration was reconstructed. The application of fluid potential analysis for hydrocarbon resource evaluation provides a new reference for studying deep hydrocarbon accumulation.

2. Geologic Background

2.1. Regional Position. The Tarim Basin is located in northwestern China and has a total area of 530,000 km^2. The Tarim Basin contains several structural zones (four depressions and three uplifts) due to multiple stages of tectonic movement during the Caledonian, Hercynian, and Himalayan orogenies [21, 22] (Figure 1(a)). The tectonic evolution consisted of six stages [22], including two intense periods of magmatic activity and volcanic eruptions in the Early Caledonian and Late Hercynian [23].

The early tectonostratigraphic evolution of the Tarim Basin involved a change from continental rift or aulacogen environment (from the Sinian to the Early Cambrian), which was related to the breakup of Rodinia, to a passive continental margin and intracratonic depression (Cambrian to Early-Middle Ordovician), and the Cambrian strata were mostly deposited on a carbonate platform in a cratonic setting [24].

A large-scale transgression took place during the Early Cambrian, resulting in the deposition of deep-water, dark mudstones at the base of the Cambrian, which are one of the main hydrocarbon source rock intervals in the basin [24]. In the late Early Cambrian, the sea level dropped significantly, and under the dry and hot climate, a shallow, evaporative basin covering an area of ~130,000 km^2 enabled the precipitation of gypsum and halite [25]. This evaporative carbonate platform setting persisted throughout the Middle Cambrian, resulting in the formation of thick gypsum and salt layers intercalated with dolostone [25]. In the Late Cambrian, the restricted basin gave way to an open carbonate platform on which thickly bedded dolostone accumulated.

The Cambrian succession consisted of six formations overlying Precambrian metamorphic basement. From bottom to top, the strata include the Lower Cambrian Yuertusi, Xiaoerbulake, and Wusonger formations; the Middle Cambrian Shayilike and Awatage formations; and the Upper Cambrian Qiulitage Formation (Figure 1(b)). Lithologically, the Yuertusi Formation is comprised of dark, organic-rich, siliceous muddy shales interbedded with phosphorites, thinly bedded dolostones, limestones, and diatomites, which were deposited in slope and basin settings [26, 27]. The Xiaoerbulake Formation consists of gray to dark gray micritic and fine-grained dolostones at the base and algal and sandy dolostones at the top, which were deposited in platform margin and interplatform reef and inner shoal settings [27]. The Wusonger Formation is dominated by gray muddy dolostones and gypsum [26, 27]. The Middle Cambrian Shayilike Formation is composed of gray limestones and dolomitic limestones, which were deposited on a platform with a high evaporation rate [26, 27]. The Awatage Formation mainly comprises gray gypsum, dolomitic gypsum, and subordinate micrite [25, 26]. The Upper Cambrian Qiulitage Formation mainly consists of gray micritic and sandy dolostones [27, 28].

2.2. Cambrian Petroleum System. The successful implementation of deep exploratory wells (Figure 1) has demonstrated that high-quality source rocks, mainly from the Cambrian system to the Lower Cambrian, were widely developed in the interplatform basin [29–31]. In addition, analysis of wells ST1, TS1, BT5, YQ6, and ZS1 revealed that many cracks and holes were developed in the Lower Cambrian Xiaorbulak Formation, the Middle Cambrian Shayilik Formation, and the Upper Cambrian Lower Qiulitage Group [32]. Based on the gypsolyte in the thick-layer zone developed in the Middle Cambrian [25], the upper, middle, and lower petroleum systems in the Cambrian system were formed in better than good Cambrian reservoir strata (Figure 1). Due to the limited distribution of the Middle Cambrian system in the Tarim basin, this study focused on the upper and lower petroleum systems.

2.3. Current Exploration Situation. There are a total of 18 wells drilled in the Cambrian strata in the Tarim Basin, and most of these drilling and logging wells have revealed indications of oil-gas in the Cambrian system. Bitumen was encountered in wells ST1 and TS1, and light oil was encountered in wells ZS1 and ZS5. Wells T 1, BT5, MB1, K2, XH 2, TS1, TS2, HT1, YQ6, ST1, WL1, LT 1, PSB2, TC1, YB1, XH1, AD1, TD1, TD2, and MC1 were mainly selected for analysis in this study.

3. Methods and Data

3.1. Source Rock Analysis. The organic matter abundance is an important parameter for evaluating source rocks, and it

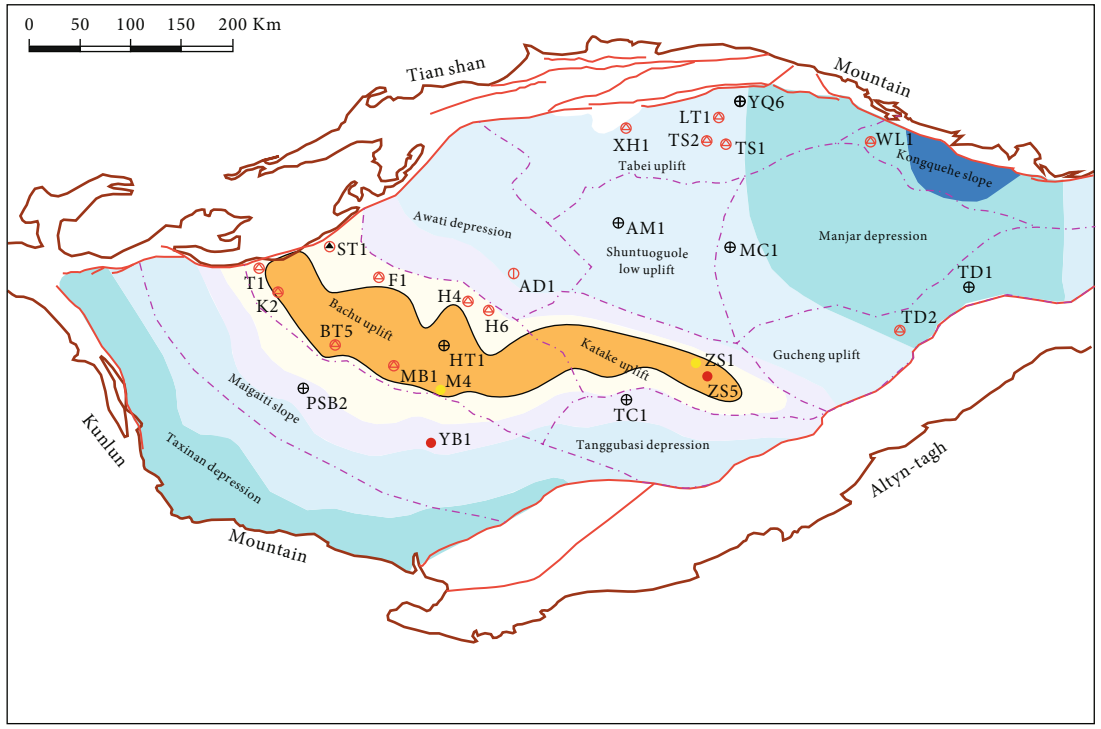

(a)

System	Series	Code	Lithology	Interf.	Petroleum system	
					Element	Subpetroleum system
Cambrian	Upper cambrian	$\epsilon_3$ql	S	T_8^0	Reservoir	Upper cambrian petroleum system
				T_8^1		
	Middle cambrian	ϵ_2a			Cap rock	Middle cambrian petroleum system
				T_8^2		
		ϵ_2s			Reservoir	
				T_8^3		
	Lower cambrian	ϵ_2w			Cap rock	Lower cambrian petroleum system
				T_8^4		
		ϵ_1x			Reservoir	
		ϵ_1y	Si		Source rock	
				T_9^0		

(b)

Figure 1: (a) Tectonic zoning and deposition of Cambrian source rocks in the Tarim Basin. (b) Division of Cambrian petroleum system in the Tarim Basin.

Table 1: Statistics of the parameters of the exploration wells in the Cambrian strata in the different tectonic zones in the Taipan Basin.

Tectonic zones	Well	Drilling depth (m)	Ro% range	TOC (%)	Lithology
Awati depression	AD 1	8087	1.8–3.0	0.8	Shale
Maigaiti slope	PSB2	7191	1.6–2.6	4.8	Shale
Tabei uplift	XH2	5856	1.3–1.4	5.5	Mudstone
Tabei uplift	TS2	6740	1.5–1.7	5.0	Carbonaceous mudstone
Tabei uplift	YQ6	7061	1.8–2.1	6.3	Carbonaceous mudstone
Kongquehe uplift	WL1	4536	1.3–1.5	2.2	Mudstone
Manjar depression	MC1	5267	3.2–3.4	6.0	Mudstone
Maigaiti slope	YB1	6618	2.0–2.4	3.0	Carbonaceous mudstone
Tanggubasi depression	TC1	5786	2.3–3.0	2.0	Mudstone

represents the potential for hydrocarbon expulsion and generation. Some scholars have measured the organic matter abundances of the source rocks in the Lower Cambrian in the Tabei uplift and have reported contents of 7–14% and up to 22.39% in local regions (Table 1) [19, 33]. The exploration activities have demonstrated that the Cambrian oil and gas in the Tarim Basin mainly came from the Lower Cambrian source rocks [20, 29, 34], but few studies have been conducted on the thermal evolution characteristics of the source rocks in the interplatform basin. Regional studies have revealed that a set of shale deposits was developed on the deep-water shelf and slope in the Lower Cambrian [35]. The cores and field profiles indicate that the organic carbon content varies from 13.89% to 22.39%, and the hydrogen index (HI) varies from 51 mg/g to 1055 mg/g.

3.2. Basin Modeling. The thermal history and oil-gas migration in the Cambrian System in the Tarim Basin were simulated using the Schlumberger PetroMod program, in which a 1D module was used for the thermal history modeling, and a 3D flow path module was used for the oil-gas migration modeling in PetroCharge program.

3.3. Modeling Methods

3.3.1. Thermal History Modeling. The purpose of modeling the thermal history was to predict the maturity and scope of the source rock in each geological period. The vitrinite reflectance is the most typical and common geochemical index of thermal evolution [36, 37]. There are many methods for recovering the thermal history, e.g., the thermometer method, the Karweil graphical method, and the Hood method. According to previous studies, the Easy%Ro chemical kinetics model (Equation (1)) is more accurate for source rocks with a middle to high degree of thermal evolution.

$$\mathrm{Ro} = xp(-1.6 + 3.7Fk), (k = 1, 2, 3, \cdots, \text{up to present}), \quad (1)$$

where Ro is the vitrinite reflectance (%) and Fk is the degree of chemical reaction at the kth burial point at the bottom stratum of the well, with a value range of 0–0.85.

3.3.2. Fluid Potential Modeling. The fluid potential concept of Hubbert has been widely quoted [4, 11] and has become a fundamental theory for studying oil-gas migration. The streamline method was used for the fluid potential modeling conducted based on Darcy's law. The flow velocity of the hydrocarbon V is as follows:

$$v = -\frac{Kk_r}{\rho} \bullet \nabla u, \quad (2)$$

where K is the permeability tensor; Kr is the relative permeability; ρ is the viscosity, and ∇_u is the overpressure gradient. The buoyant force is the driving force and satisfies $|\nabla u| = (\rho_w - \rho_p) \times g$, where ρ_w and ρ_p are the densities of water and oil, and $g = 9.80665\,\mathrm{m/s^2}$. Generally, the streamline method reveals the migration and accumulation trends from the source rocks to the traps. The streamline length represents the distance of the fluid migration and accumulation. The streamline accumulation indicates that the oil and gas are trapped along the dominant migration channel. In this fluid potential simulation, the Lower Cambrian source rocks were characterized by the bottom interface of source rocks T90. The trap was characterized by the structural morphology of the reservoir'stop surface, the Lower Cambrian petroleum system trap was selected as the reservoir's top interface T84, and the upper interface was T80.

3.4. Selection of Single Wells for Modeling. In this study, nine exploratory wells in different tectonic units in the study area were selected for hydrocarbon generation and expulsion history modeling. Well AD2 in the Awati depression; well MS1 in the west Manjar depression; wells XH1, TS2, and YQ6 in the Tabei uplift; well WL1 in the Kongquehe uplift; well MC1 in the Manjar depression; well TC1 in the Tanggubasi depression; and well YB1 in the Maigaiti slope were selected for thermal evolution modeling.

3.5. Formation Framework and Lithological Parameters. Based on the formation sequence of a single well in the study area [38], the current formation interface was focused on, and a formation framework at different geological times was constructed based on the geologic chronology. Based on the analysis of the single-well data, the selected single wells were commonly drilled below the Ordovician strata, and for the wells that did not reach the Cambrian system, the formations were estimated based on seismic data for

Table 2: Formation sequence framework for the exploratory wells in different tectonic zones in the interplatform basin.

Tectonic zones	Well name	Formation sequence framework (m)											
		Q–E	K	J	T	P	C	D	S	O	ϵ_3	ϵ_2	ϵ_1
Awati depression	AD 1	3283	3518	3518	4320	5456	5888	6090	7167	8266	*9192	*9792	*10376
Maigaiti slope	PSB2	4412	4412	4412	4412	5779	6538	6757	6891	7191	*7296	*7491	*7951
	XH1	5267	5763	5763	5763	5763	5763	5763	5763	5763	5763	5763	5856
Tabei uplift	TS2	3355	4443	4504	4954	4954	5520	5520	5520	6740	*6950	*7460	*7935
	YQ6	3755	4900	5026	5435	5435	5660	5671	7061	7235	*7611	*8361	*8760
Kongquehe uplift	WL1	1704	2348	3279	3279	3279	3279	3279	3279	3940	4175	4353	4536
Manjar depression	MC1	1320	1531	2356	2774	3410	4001	5266	6675	8750	*13040	*13790	*14340
Tanggubasi depression	TC1	2201	2569	3023	4104	4794	4794	4794	5122	5786	*6936	*7586	*7806
Maigaiti slope	YB1	3607	3749	3749	3749	4521	5020	5593	5593	5718	*7173	*7631	*7931

Note: * indicates estimated data.

Table 3: Statistics of the erosion thickness of the formations in the different exploratory wells in the Bachu–Tabei uplift (from the Sinopec Northwest Petroleum Exploration and Production Research Institute).

Well	Formation											
	K	J	T	P	C	D	S	O_{2-3}	O_1	ϵ_3	ϵ_2	ϵ_1
AD1	475		515	1120	70		700	480				
TC1	155		225	750			110					
YB1	230		85	550			125	1105	185			
PSB2	220		5	450			1000	830	120			
AM1	30		356	1250			350	720				
XH1	550		600	160	430	26	1230	550	70	210	105	475
TS2	150	106	500	320	106		1123	500				
YQ6	200	85	510	110	250		820	400				
YL1	120	5	400	50	270		1190	470				
MC1	130	95	350	1520								

the reference region (Table 2). The interpreted relevant seismic data were mainly obtained from the Sinopec Exploration and Development Research Institute.

The key to properly calibrating the formation compaction and objectively recovering the burial history of the deposits is to correctly select the lithological parameters of the formation. Based on the drilling data and logging data for single wells, the lithology of each formation and its percentage content was calculated. The mixed lithology was mixed from the standard lithology using a certain percentage based on the calculation results. The thermal conductivity and compaction coefficient were set as the default values of the model.

3.6. Recovery of Erosion Thickness. The erosion thickness is a critical factor in recovering the burial history. Multiple uplift events occurred in the Tarim Basin, resulting in 9 unconformities (Figure 1(b)): the Cretaceous (T40), Triassic (T50), Carboniferous (T57), Upper Devonian (T60), Silurian (T70), Upper Ordovician (T72), Middle Ordovician (T74), Upper Cambrian (T81), and Lower Cambrian (T90) unconformities. The erosion data are partially from the Northwest Oilfield Company Research Institute Foundation Institute, and they mainly include the erosion thicknesses of the Ordovician, Silurian, Devonian, Carboniferous, Permian, Triassic, Jurassic, and Cretaceous formations. According to the data statistics, the amounts of erosion of the Ordovician, Silurian, and Permian formations were large (Table 3).

3.7. Boundary Conditions

3.7.1. Paleo-Geotemperature. The surface temperature includes the current temperature and the paleo-geotemperature. Although there is a difference in the current surface temperature in the Tarim Basin, the difference is small, and the surface temperature is often taken as 18°C [15]. The background value of the paleo-geotemperature is usually set using a customized Wygrala (1989) model in PetroMod. The Tarim Basin is located in the Eastern Asian Plate (39°N) in the Northern Hemisphere. Owing to the variations in the geologic age, the paleo-geotemperature usually varies from 16°C to 30°C (Figure 2).

3.7.2. Paleowater Depth. Paleowater depth analysis is important and significant for reconstructing the

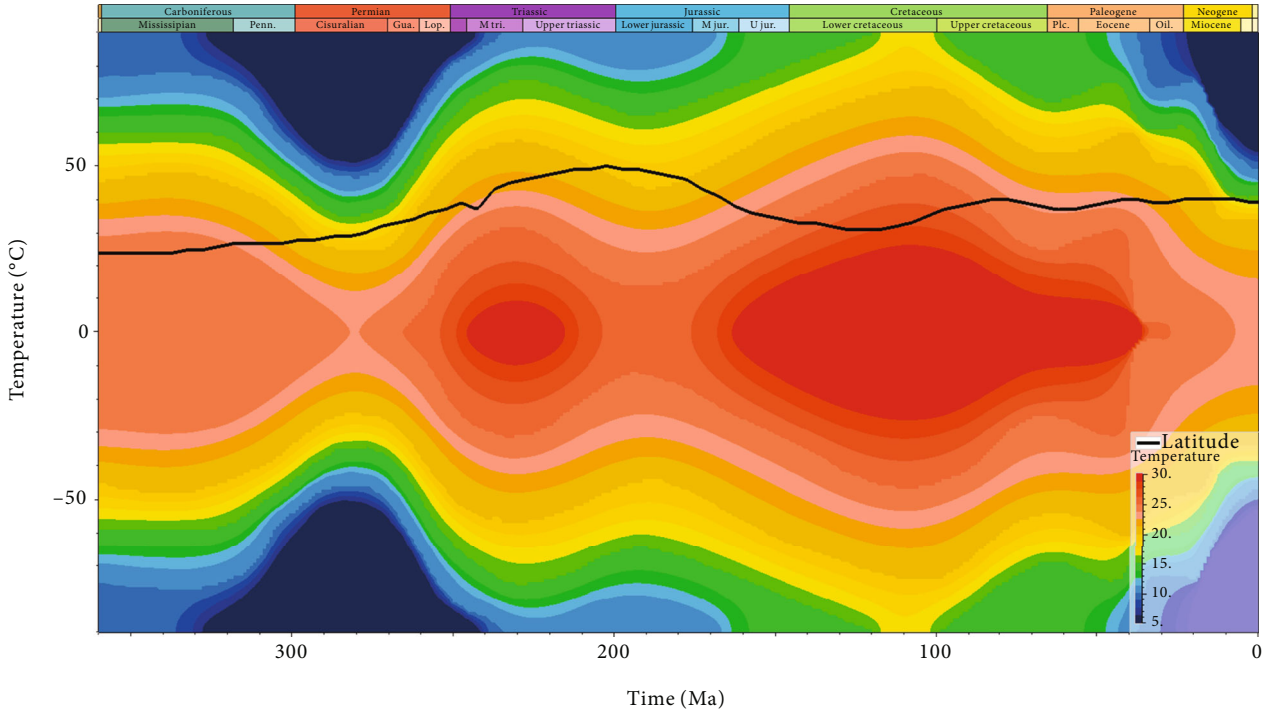

Figure 2: Variations in the surface temperature of the Central Asian plate (39°N) in the Northern Hemisphere.

Table 4: Ancient water depth in the Tarim Basin in each geological period.

Geologic age	Main sedimentary environment	Paleowater depth (m)
T-Q	Bathyal lake, shallow lake, river	0–45
S-P	Shallow sea, tidal flat, river delta	0–130
$O_{2\text{-}3}$	Bathyal sea, shallow sea, open platform	0–500
$\in$-$O_{1\text{-}2}$	Deep sea, shallow sea, restricted platform	10–930

paleoenvironment, basin structure, and evolution [39]. In this study, the paleowater depths in the different regions were mainly calibrated based on the sedimentary history of the Tarim Basin and the uplift trend of its elevation (Table 4).

3.7.3. Paleoheat Flow. The Paleozoic heat flow is the product of the geothermal gradient and the thermal conductivity of the rocks. Different tectonic evolution pathways result in different Paleozoic heat backgrounds [37]. The thermal conductivities of the main lithologies of the different strata were obtained based on a field core thermal conductivity test (Table 5). The geothermal gradient in the platform basin was found to be between 3.37 and 1.9°C/100 m via drilling temperature measurements in the reference area (Table 6), and it has exhibited a decreasing trend since the Cambrian. The results are as follows: 34–44 mW/m^2 in the Cambrian–Ordovician, 40–56 mW/m^2 in the Silurian–Devonian, 41–78 mW/m^2 in the Carboniferous–Permian, 39–76 mW/m^2 in the Triassic–Cretaceous, 35–65 mW/m^2 in the Cenozoic, and 34–55 mW/m^2 at present. The evolution of the heat flow was as follows: low in the Early Paleozoic, high from the Late Paleozoic to the Mesozoic, and low at present, which is consistent with the results of previous studies [40, 41].

3.7.4. Paleostructural Restoration. The evolution of the ancient structure has a great influence on secondary hydrocarbon migration and accumulation. The stratum stripping method uses the compaction curve to restore the paleothickness of the stratum [42, 43]. In the calculation, the paleoelevation depth (HSL) of the corresponding structural surface is usually considered to be the sum of the tectonic depth (-Hd) in the historical period relative to the historic sea level and the denudation thickness (Hb) before the historical period [44]. Therefore, the ancient elevation depth (HSL) at any point in the basin can be expressed as follows:

$$H_{SL} = -H_d + H_b. \tag{3}$$

In this study, the ancient structures of the Lower Cambrian interface (T_{84}) and the Upper Cambrian interface (T_{80}) were recovered.

3.8. Fluid Potential. The fluid potential is an important reference parameter for studying the direction and channel of secondary oil-gas migration [11, 45–47]. In this study, the latest Schlumberger PetroCharge model was combined with

Table 5: Thermal conductivities of different lithologies in the Tarim Basin.

Formation	O	O	S	D	C	P	T	J	K	E	N
Lithology	Limestone	Dolostone	Sandstone	Limestone	Silty mudstone	Silt	Sandstone	Sandstone	Mudstone	Silt	Silt
Thermal conductivity	2.13	2.33	2.10	2.13	1.90	1.90	2.10	2.10	2.06	2.02	2.21

Table 6: Statistics of drilling temperature measurements in the Tarim Basin.

Well	YB1	PSB2	XH2	TC1	YQ6	TS1	ZS1	TD1
Temperature (°C)	141.3	161	106	160	157	170	130	98.3
Depth (m)	4900	5852.76	5125	7200	7510	8810	4600	2919.72
Geothermal gradient (°C/100 m)	2.88	2.75	2.07	2.22	2.09	1.93	2.83	3.37

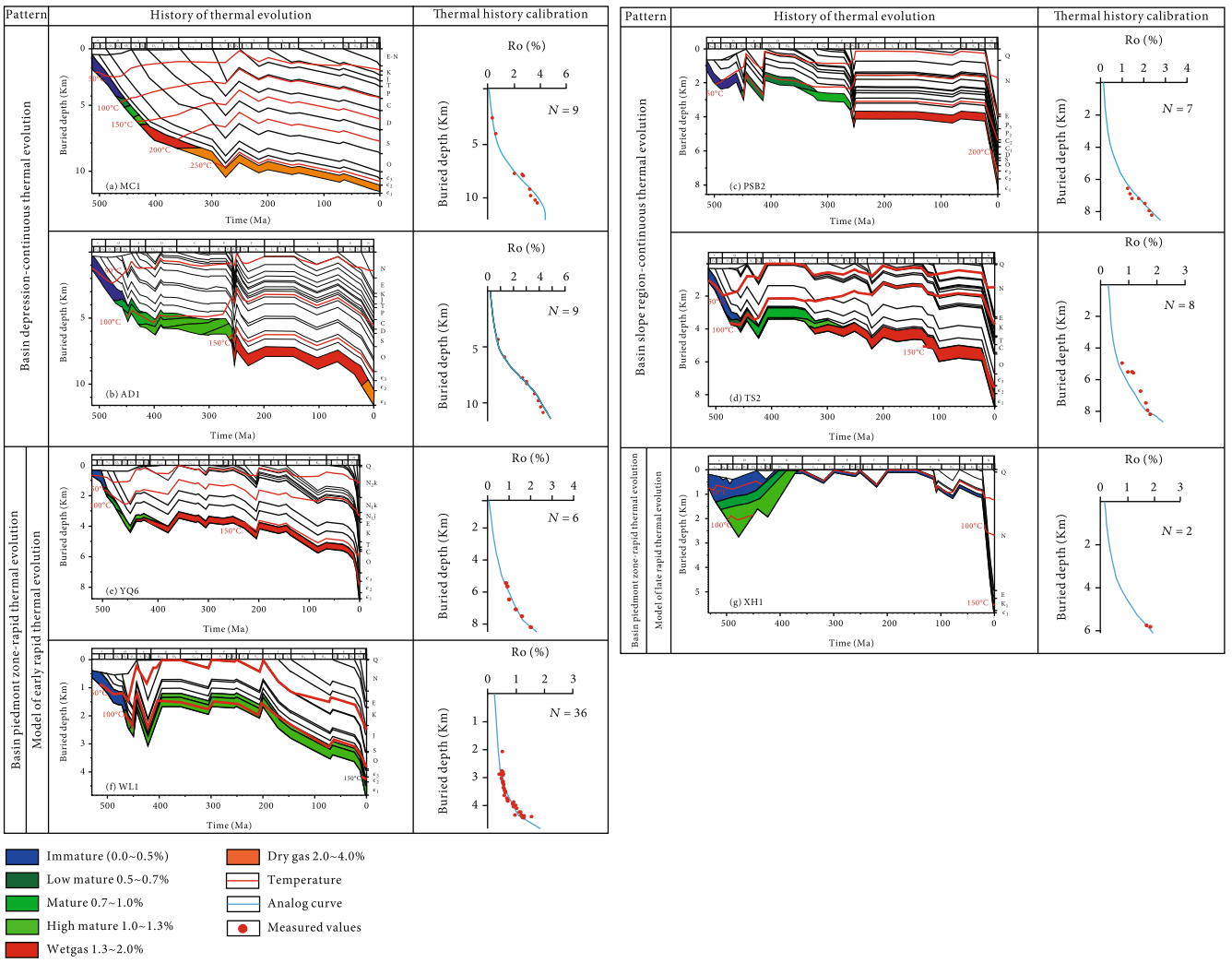

Figure 3: Thermal evolution of the Lower Cambrian source rocks in the Tarim Basin. (Note: the depth of the modeling well is the bottom depth of the Cambrian strata and is not the actual drilling depth.)

the paleostructure and maturity of the source rocks to calculate the paleofluid potential and to explore the fluid charging and migration in both the Upper and Lower Cambrian petroleum systems in the Tarim Basin to determine the migration and accumulation characteristics of the ultradeep oil-gas system in the basin.

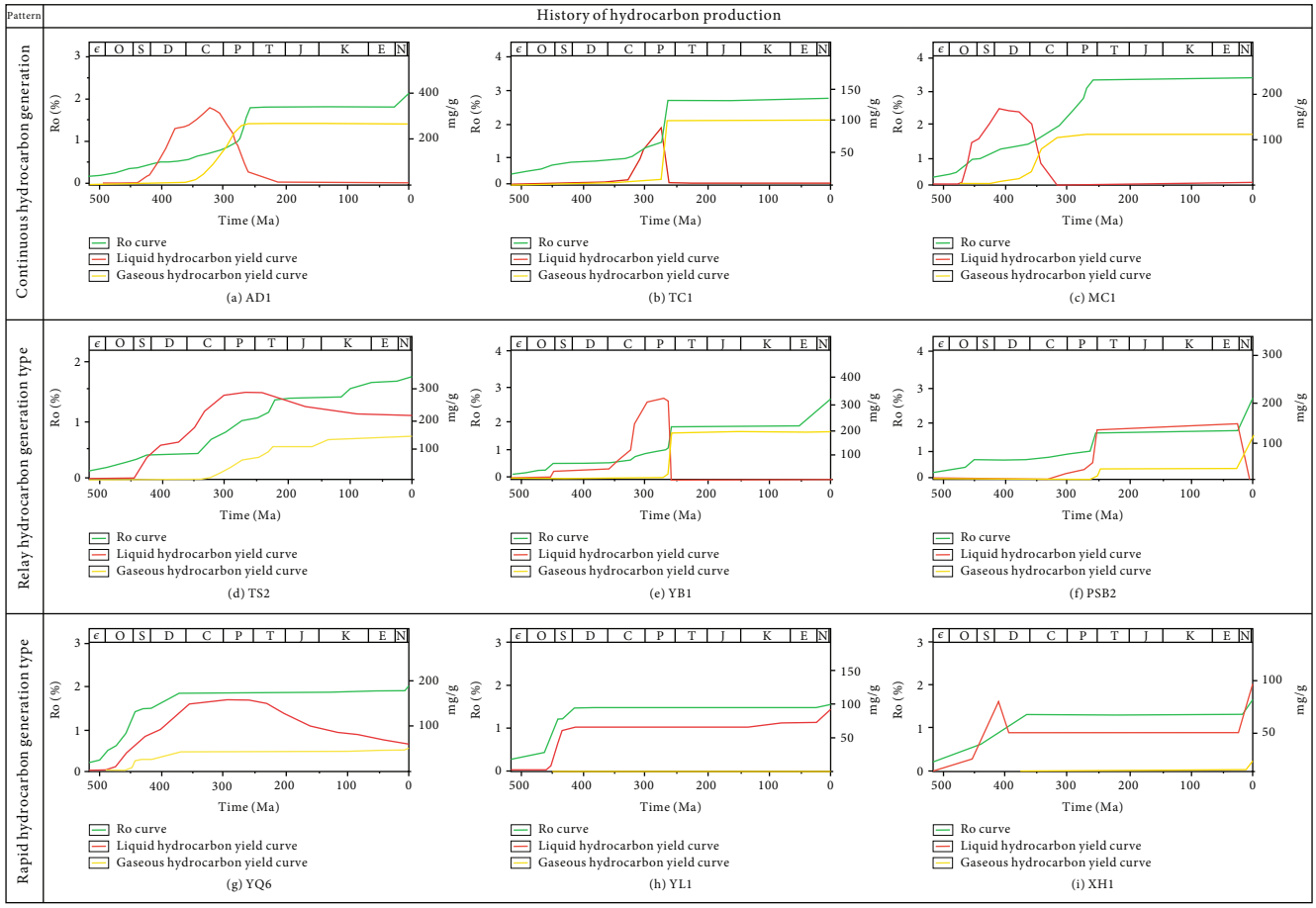

Figure 4: The thermal and hydrocarbon generation history of the Lower Cambrian source rocks in the Tarim Basin.

4. Results

4.1. Thermal Evolution of Lower Cambrian Source Rocks

4.1.1. Model of Thermal Evolution. The purpose of thermal history modeling is to reconstruct the thermal history of the sedimentary formation in the basin, which is an important basis for analyzing the temperature and maturity of the hydrocarbon source rock in each geological period [37, 40]. In this study, nine exploratory wells in five of the major tectonic units in the interplatform basin were selected as representative of the geological background. These wells were used to recover the partial Cambrian thickness values and to create a model of the thermal evolution of a single well constrained by the vitrinite reflectance (Table 1) in the Paleozoic based on the related paleoheat flow values for the reference regions. According to the model of the thermal evolution of the basin, the Lower Cambrian source rocks in the interplatform basin experienced different thermal evolutions (Figure 3), and the following three thermal evolution models were developed. (1) The continuous hydrocarbon generation model is the representative wells that include wells AD1, TC1, and AM1. Owing to the influence of the continuous settling, the thermal evolution of the source rocks was characterized by a continuous increase in temperature. The vitrinite reflectance varies from 1.3% to 4%. Overall, it is in the mature stage and is mainly developed in the basin depression. (2) The continued hydrocarbon generation model is the representative wells that include wells TS2 and PSB2. The hydrocarbon generation process occurred during stages of temperature increase. The vitrinite reflectance varies from 0.7% to 4%. Overall, it is in the mature to overmature stage and is mainly developed in the slope. (3) The fast hydrocarbon generation model is the representative wells that include wells WL1 and YQ6. The thermal evolution of the source rocks began from the Cambrian to the Silurian–Devonian and then entered a lag phase, undergoing an early rapid increase in temperature and a later lag in the temperature increase. The vitrinite reflectance varies from 0.7% to 1.3%. Overall, it is in the mature to over-mature phase and mostly occurs in the mountain front. The representative well of the late fast thermal evolution model is well XH1. The thermal evolution rate increased rapidly after the Miocene, i.e., the late fast thermal evolution model.

4.1.2. Hydrocarbon Generation Model. In this study, the hydrocarbon generation and expulsion histories of nine exploratory wells in the different tectonic zones in the study area were reconstructed (Figure 4) based on the hydrocarbon generation history of the Lower Cambrian source rocks in the different tectonic zones. Three hydrocarbon

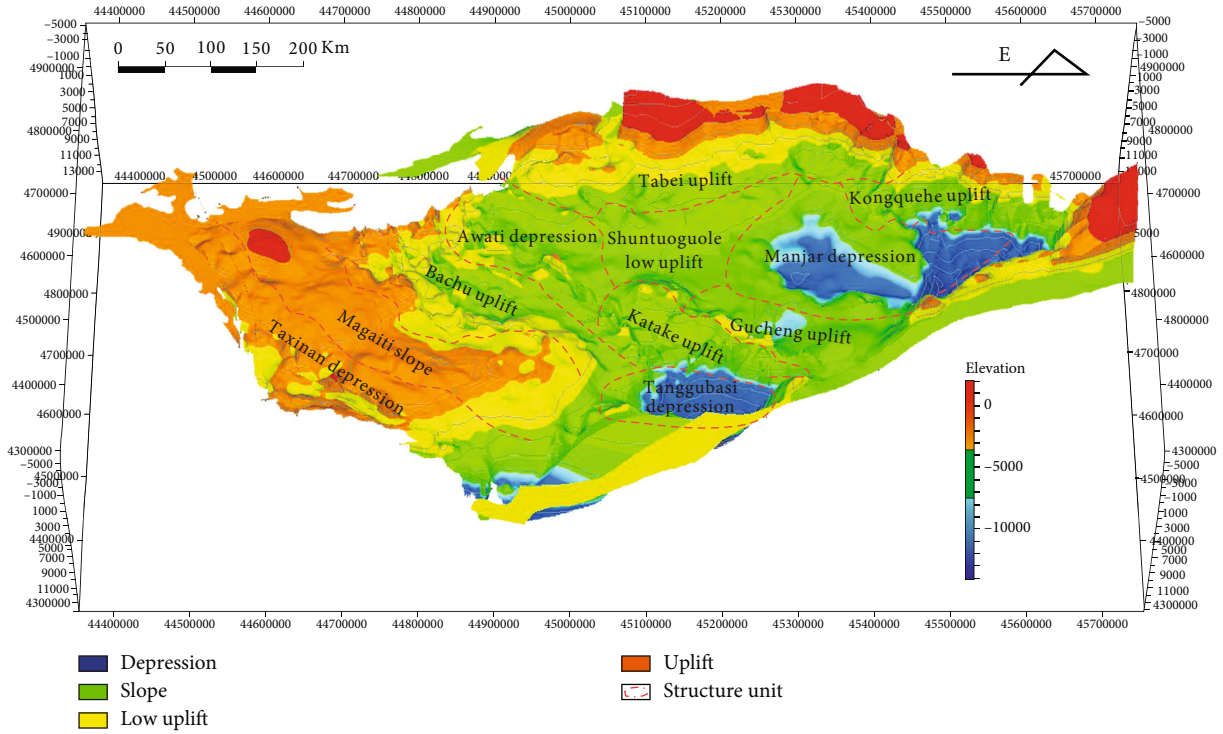

(a) Middle Caledonian

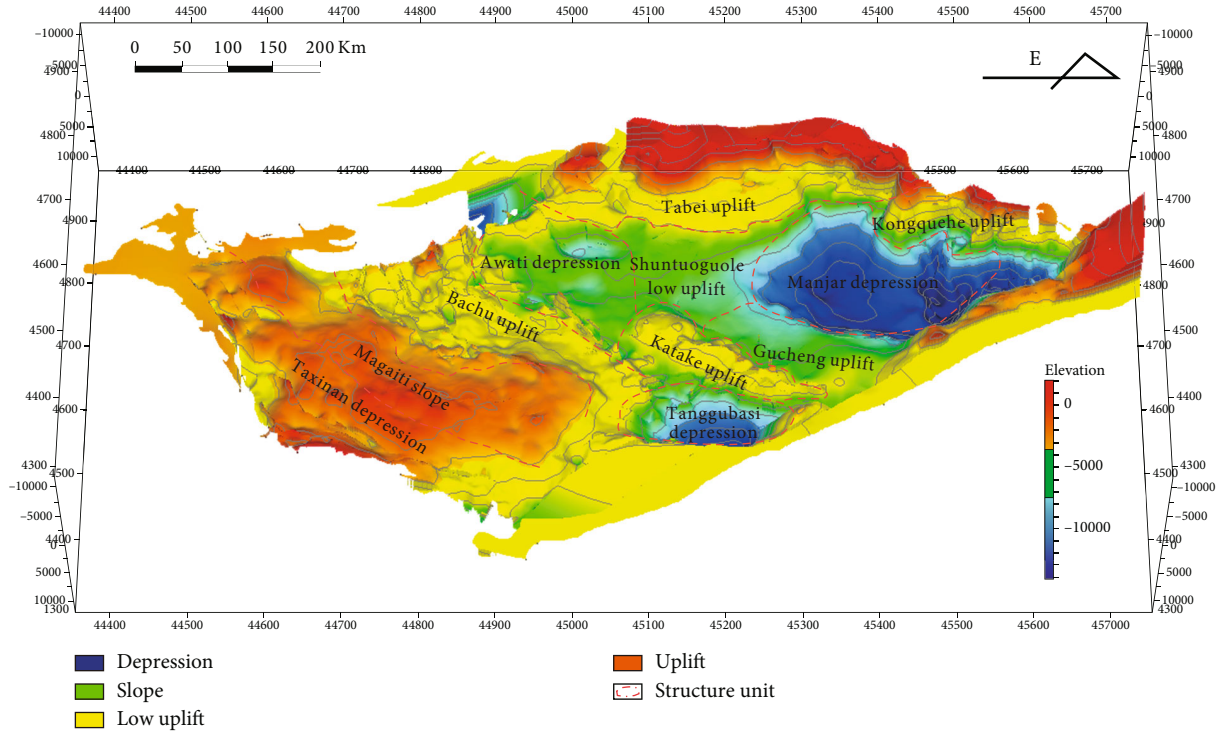

(b) Late Caledonian

Figure 5: Continued.

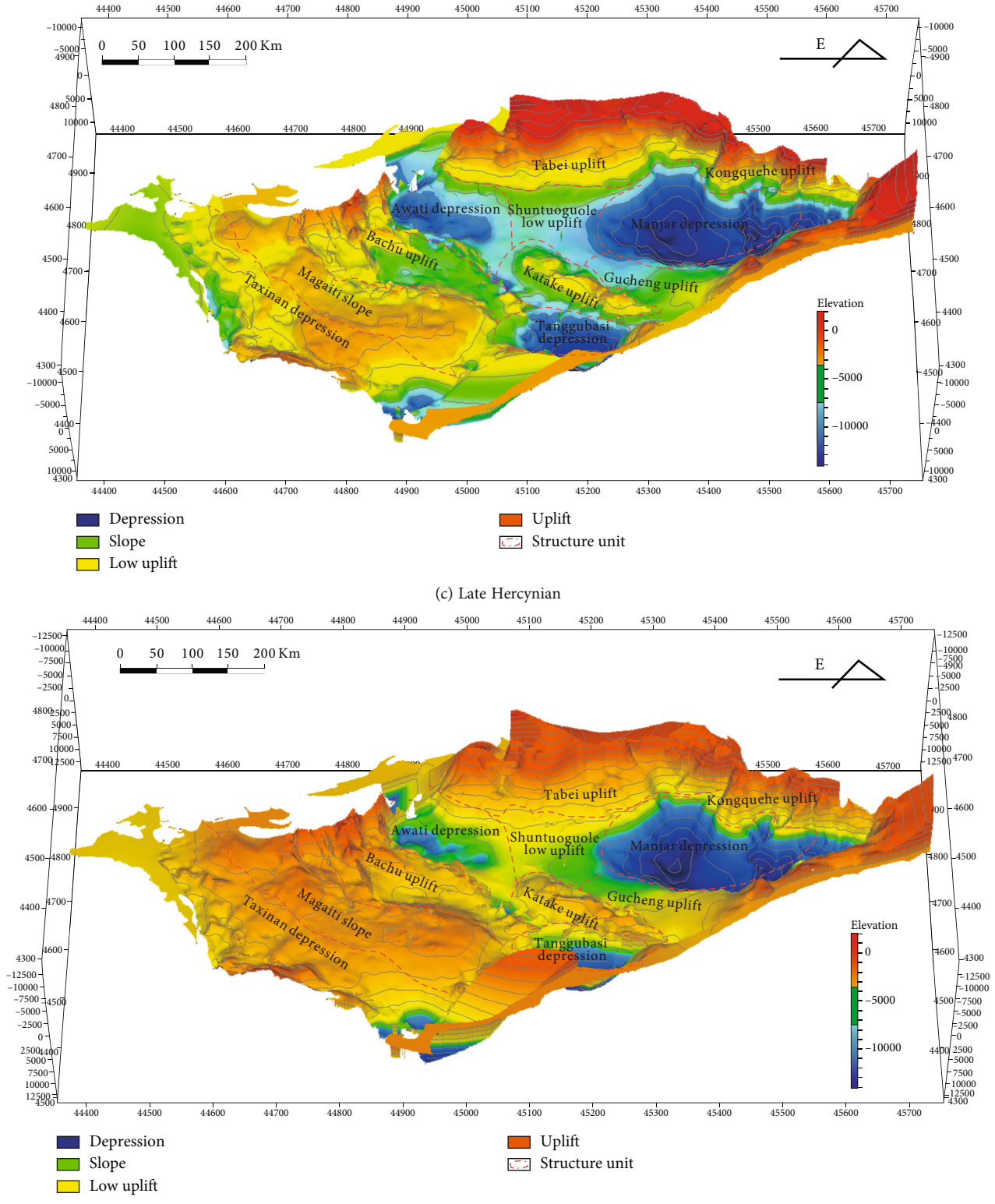

(c) Late Hercynian

(d) Late Himalayan

Figure 5: Paleotectonic restoration of the Lower Cambrian in the Tarim Basin.

generation and expulsion models were developed for the Lower Cambrian strata in the interplatform basin. (1) The continuous hydrocarbon generation model is the representative wells that include wells AD1, TC1, and AM1. The hydrocarbon generation began in the Late Ordovician. The peak period of liquid hydrocarbon generation was from the Devonian to the Carboniferous, and the peak period of gas generation occurred in the Early Permian. The hydrocarbon generation process was continuous. (2) The continued hydrocarbon generation model: the representative wells

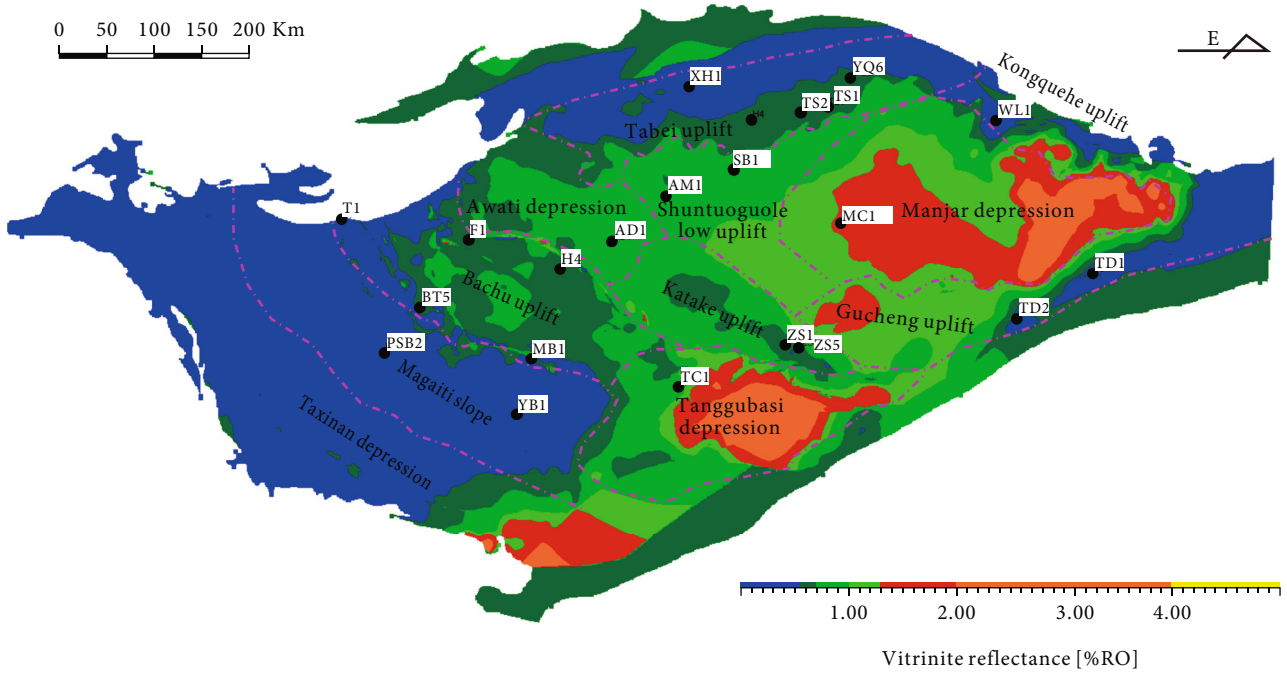

(a) Middle Caledonian

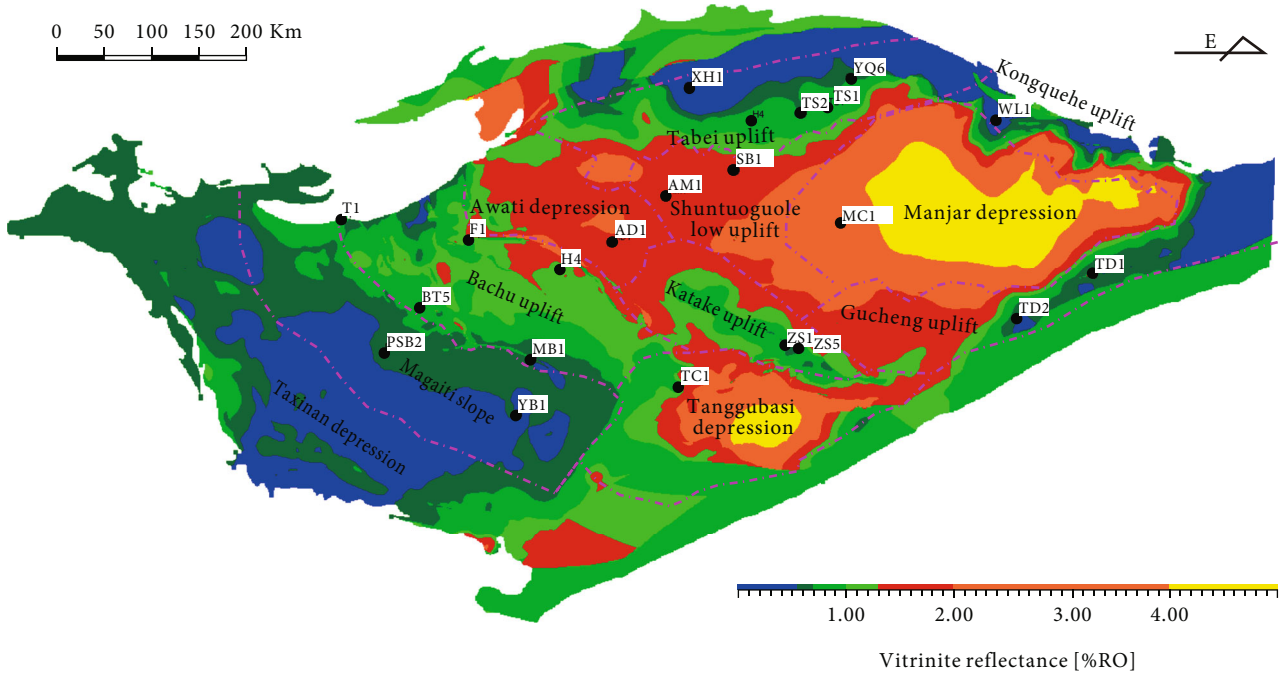

(b) Late Caledonian

Figure 6: Continued.

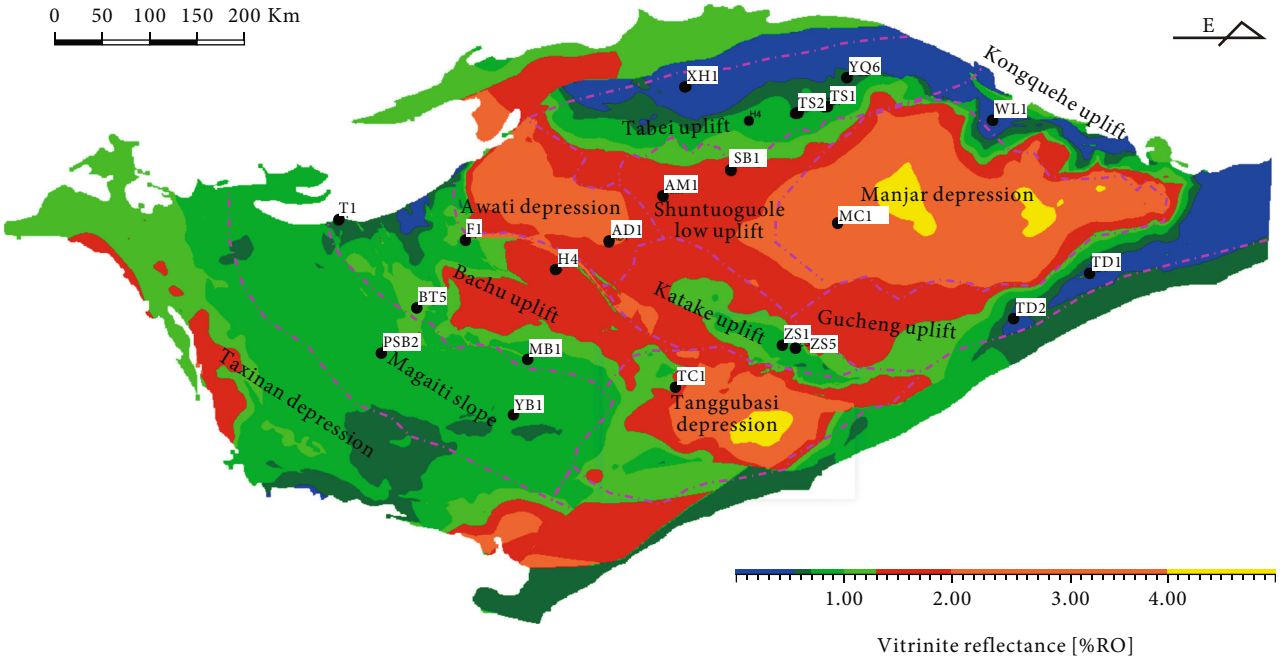

(c) Late Hercynian

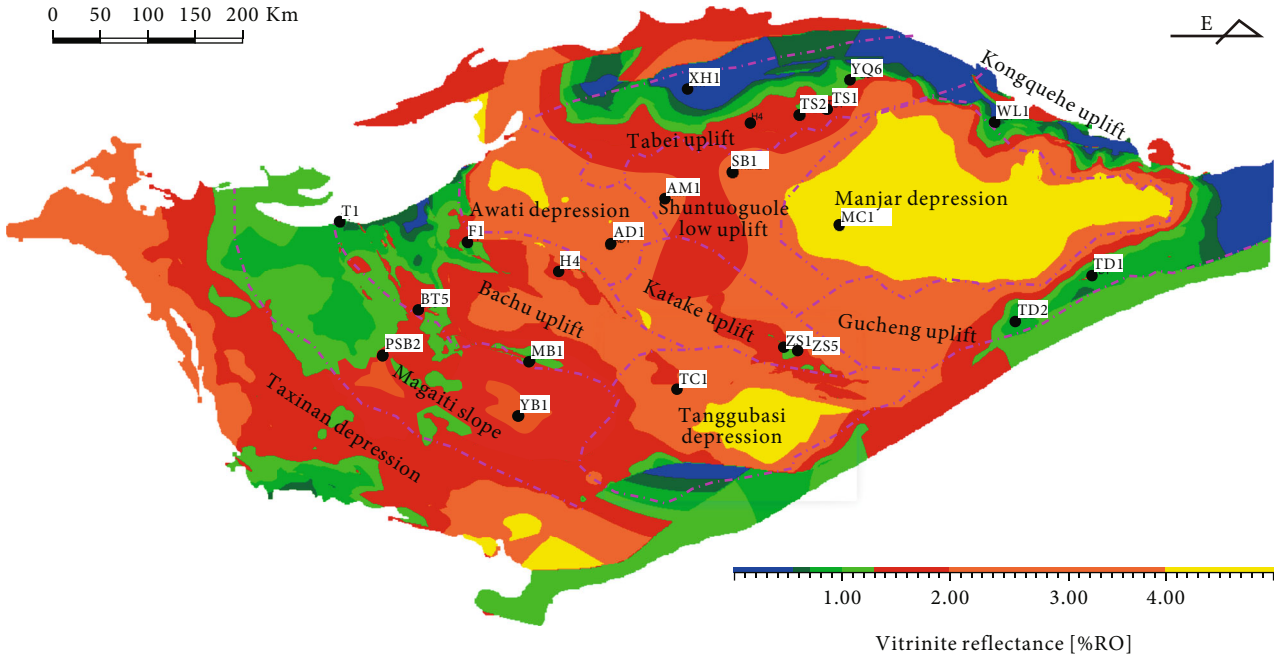

(d) Late Himalayan

Figure 6: Thermal evolution of the Lower Cambrian source rocks in the Tarim Basin (seismic T90 interface).

include wells TS2 and PSB2. The hydrocarbon generation began in the Late Ordovician. The peak period of hydrocarbon generation occurred in the Late Carboniferous, the peak period of liquid hydrocarbon generation occurred in the Permian, and the peak period of gaseous hydrocarbon generation occurred in the Triassic. The hydrocarbon generation occurred in stages. (3) The fast hydrocarbon generation model is the representative wells that include wells WL1 and YQ6. The thermal evolution of the source rocks occurred from the Cambrian to the Silurian–Devonian and then entered a lag phase. Owing to the relatively low degree of thermal evolution, this was the early fast hydrocarbon generation model. For example, in well XH1, a rapid increase in the degree of thermal evolution occurred after the Miocene, and the peak of oil and gas generation was reached, i.e., the late fast hydrocarbon generation model. Overall, the Lower Cambrian source rocks in the Tarim Basin were characterized by early oil generation and late gas generation, and the hydrocarbon generation history was different in the different regions.

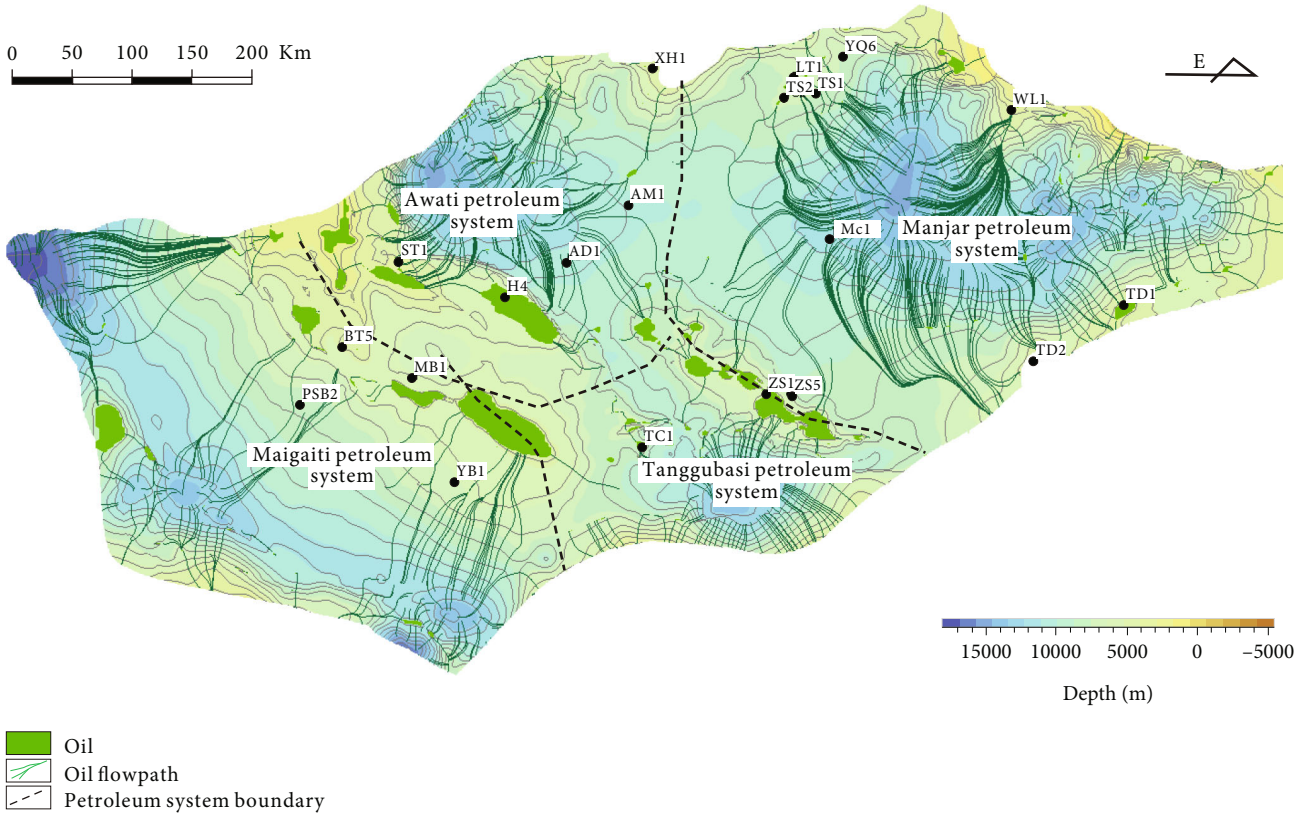

(a) Middle Caledonian

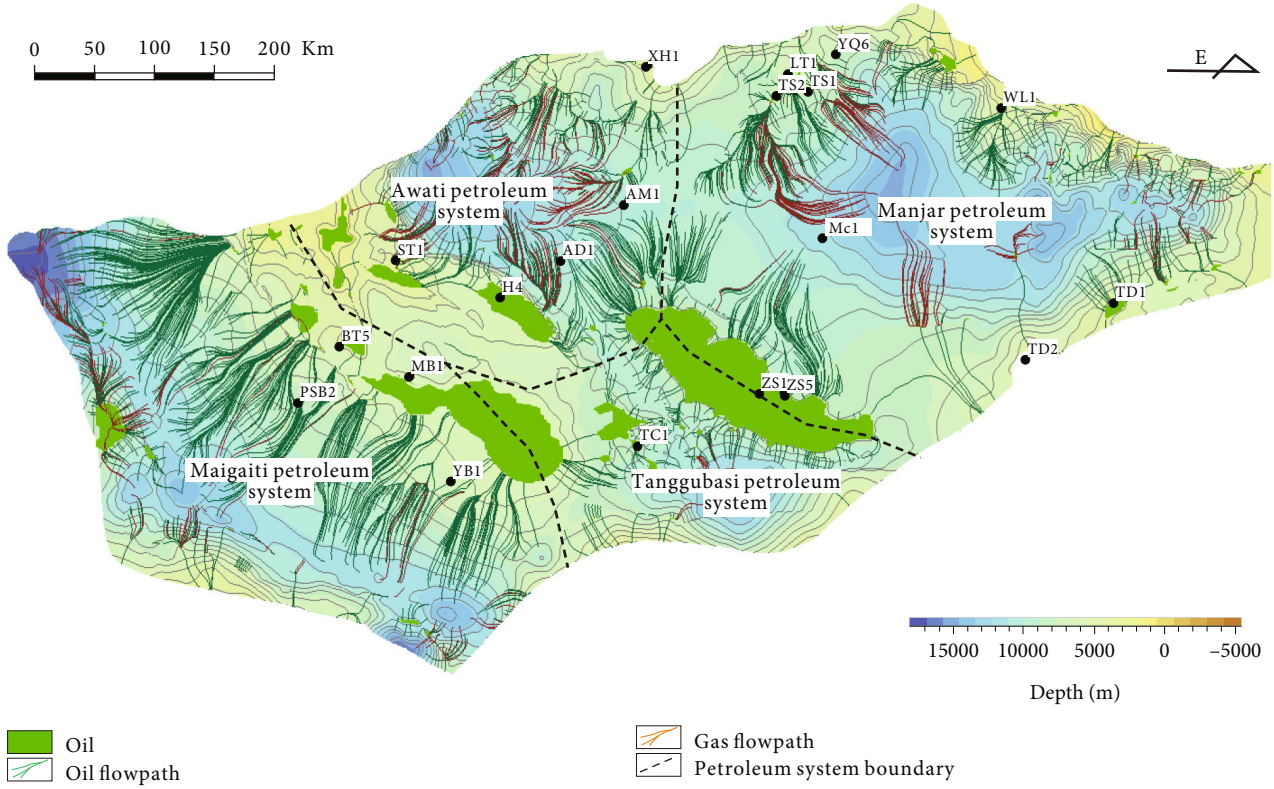

(b) Late Caledonian

Figure 7: Continued.

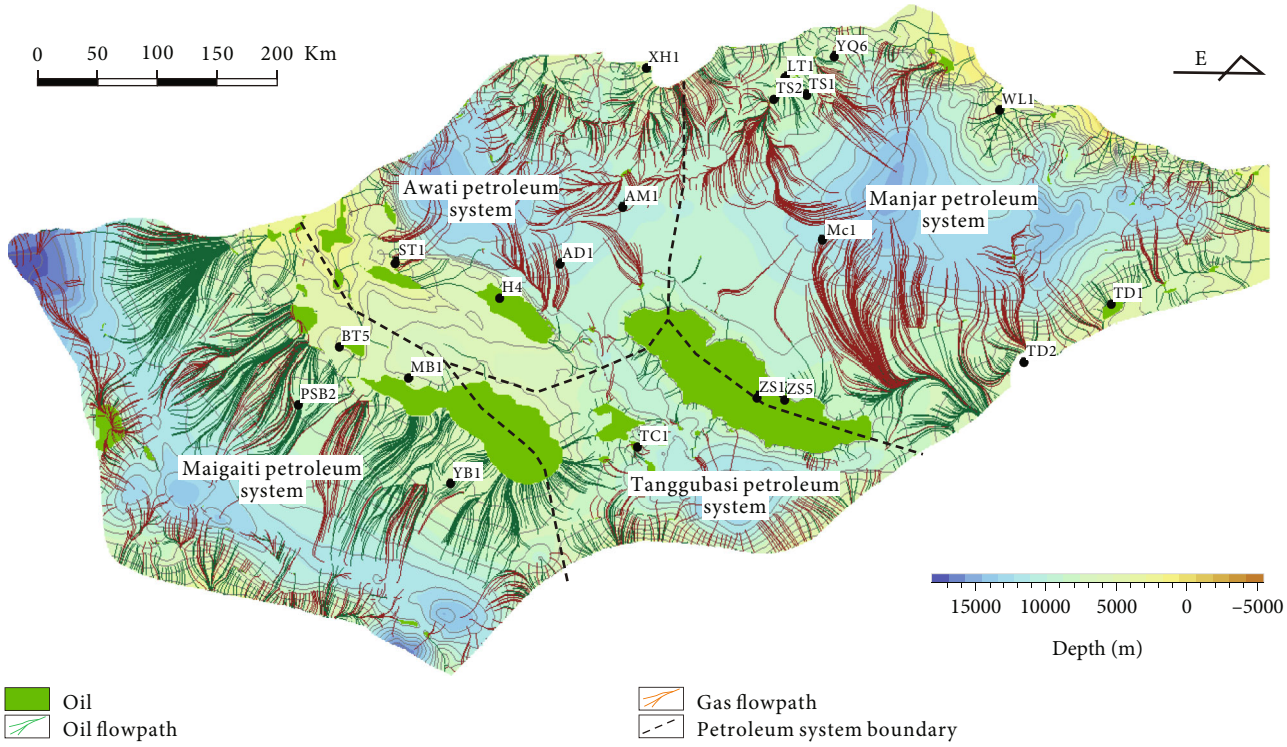

(c) Late Hercynian

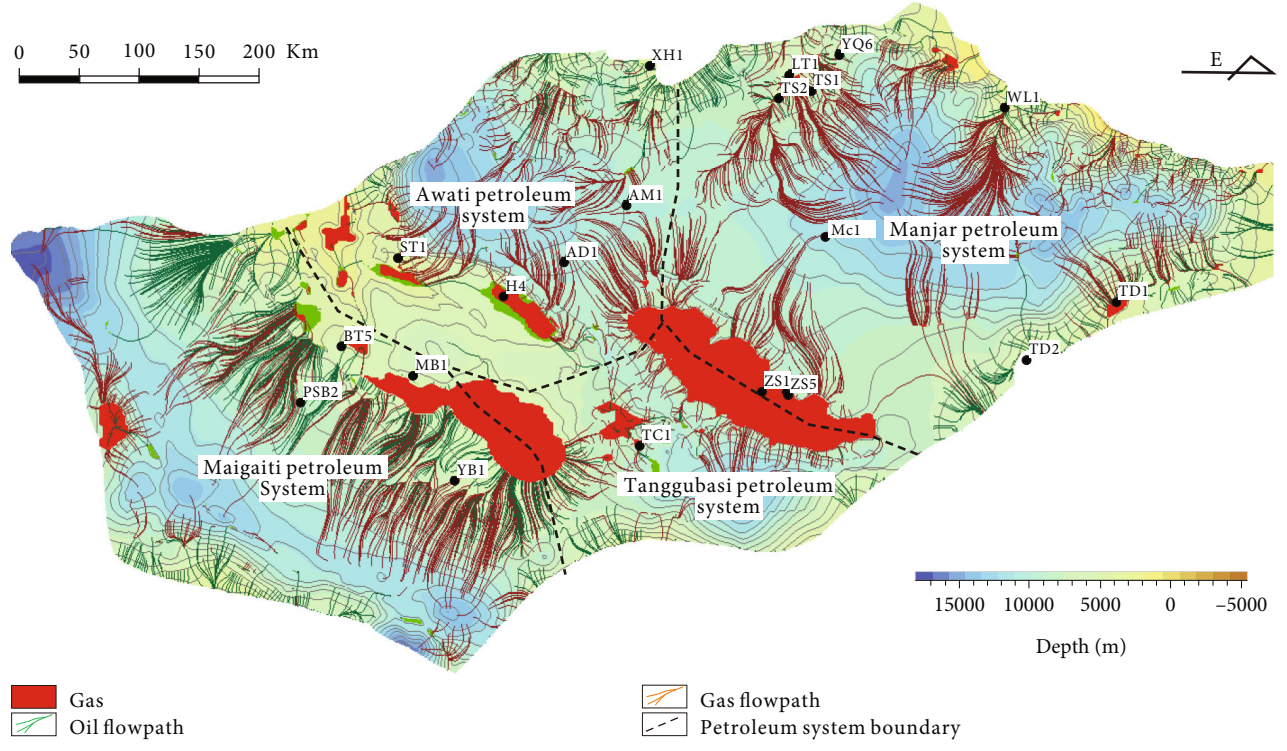

(d) Himalayan

Figure 7: Streamline distribution of the lower petroleum system (T90–T84) in the Tarim Basin.

4.2. Oil-Gas Migration and Accumulation Trends of the Petroleum System. Based on the description of the current formation structure in the basin, the paleostructure of T90 in the Lower Cambrian during four critical period (e.g., the Middle Caledonian, Early Hercynian, Late Hercynian, and Late Himalayan) was recovered (Figure 5). It can be seen from Figure 6 that in the Lower Cambrian, the Tarim Basin experienced long-term tectonic subsidence, but there were

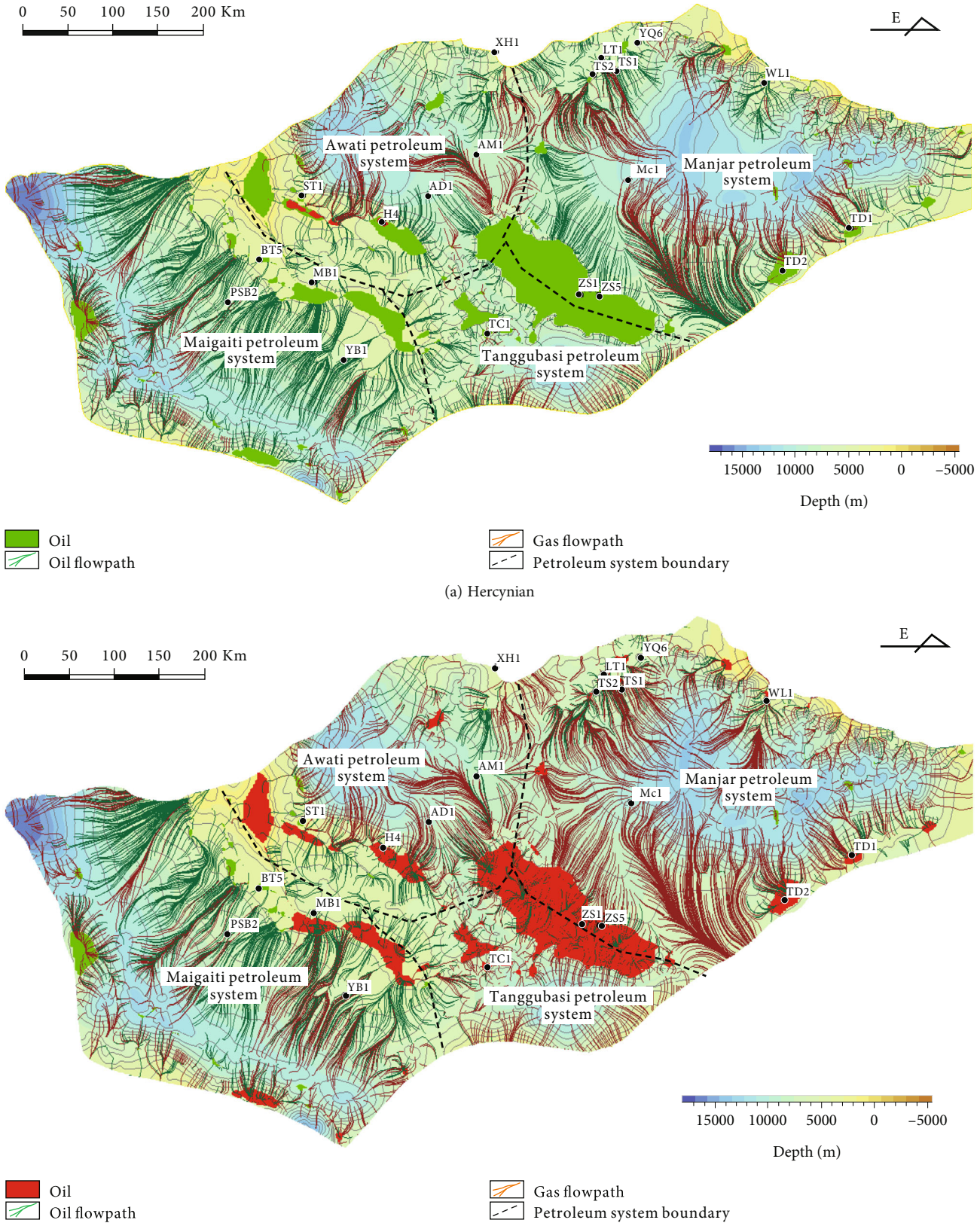

Figure 8: Streamline distribution of the lower petroleum system (T90–T80) in the Tarim Basin.

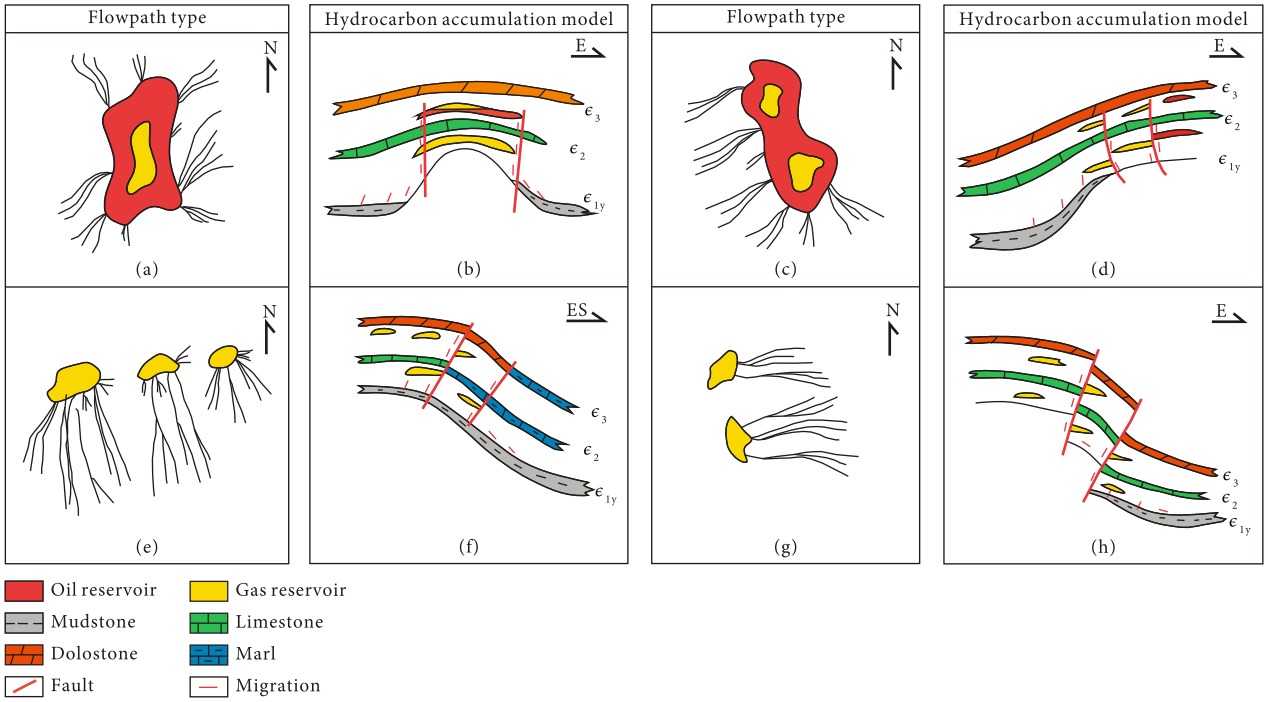

Figure 9: Models of Cambrian oil-gas charging in the Tarim Basin.

obvious differences under the influence of the structure of the basin's base and tectonic compression. Among them, the Manjar depression and Tanggubasi depression have been depressions for a long time, and their scope has been expanding. The Awati depression began to rapidly settle in the Late Hercynian. The Bachu area consists of a monocline that is high in west and low in east and developed between the Caledonian and Early Hercynian. After the Late Hercynian, it was compressed by the NE trending structure, and the structure reversed, producing an uplift and depression pattern that was low west and high east. The above reconstruction of the tectonic evolution is consistent with the results of a previous study [48].

Based on the evolutionary characteristics of the paleostructure, the characteristics of the thermal evolution of the source rocks in the Lower Cambrian system during four critical period (i.e., Middle Caledonian, Late Caledonian to Early Hercynian, Late Hercynian, and Late Himalaya) were reconstructed using the PetroMod software, and the results are consistent with the thermal evolutions of the single wells (Figure 6).

According to the thermal evolution of the Lower Cambrian source rocks (Figure 7), the Lower Cambrian source rocks in the Manjar depression, Tanggubasi depression, and Awati depression in the interplatform basin entered the mature stage as a whole in the Middle Caledonian (Figure 6(a)) and provided the material foundation for the development of the paleo oil reservoir in the Caledonian. From the Late Caledonian to Early Hercynian, the Lower Cambrian strata underwent rapid thermal evolution due to continuous sedimentation, and the source rocks in the interplatform basin entered the mature-highly mature stage as a whole, providing oil-gas sources for the oil-gas reservoir in the Hercynian (Figure 6(b)). In the Late Hercynian, the Lower Cambrian source rocks in the interplatform basin entered the mature to overmature stage, and the thermal evolution of the source rocks succeeded the characteristics in the Early Hercynian, during which the source rocks in the Maigaiti slope entered the mature stage as a whole (Figure 6(c)). In the Himalayan, the Lower Cambrian source rocks in the interplatform basin entered the highly maturity stage and had already been in the overmature stage in the depression (Figure 6(d)), resulting in late gas migration in the interplatform basin.

Overall, the thermal evolution of the Lower Cambrian source rocks in the interplatform basin was greatly different in the different regions. That is, the degree of thermal evolution was the highest in the Manjar depression and lagged in the Maigaiti slope and southwestern depression in the Tarim Basin. The overall trend was early in the east and late in the west. Within the same tectonic unit, the vitrinite reflectance of the hydrocarbon source rocks varied, e.g., in the Shuntuoguole low uplift and the Maigaiti slope, which is an important reason for the existence of multiphase oil-gas reservoirs in the interplatform basin. The northern Tarim slope, Shuntuoguole low uplift, and Maigaiti slope had an overall source rock maturity of less than 2%, i.e., the high-maturity stage. Owing to their large hydrocarbon generation potential, they are promising targets for deep oil-gas exploration.

4.3. Oil-Gas Accumulation in the Lower Petroleum System. In this study, the thermal evolution characteristics of the source rocks, reservoir physical properties, and trap evolution characteristics were used to reconstruct the fluid migration in the different periods in the oil-gas systems (Figures 7 and 8). In

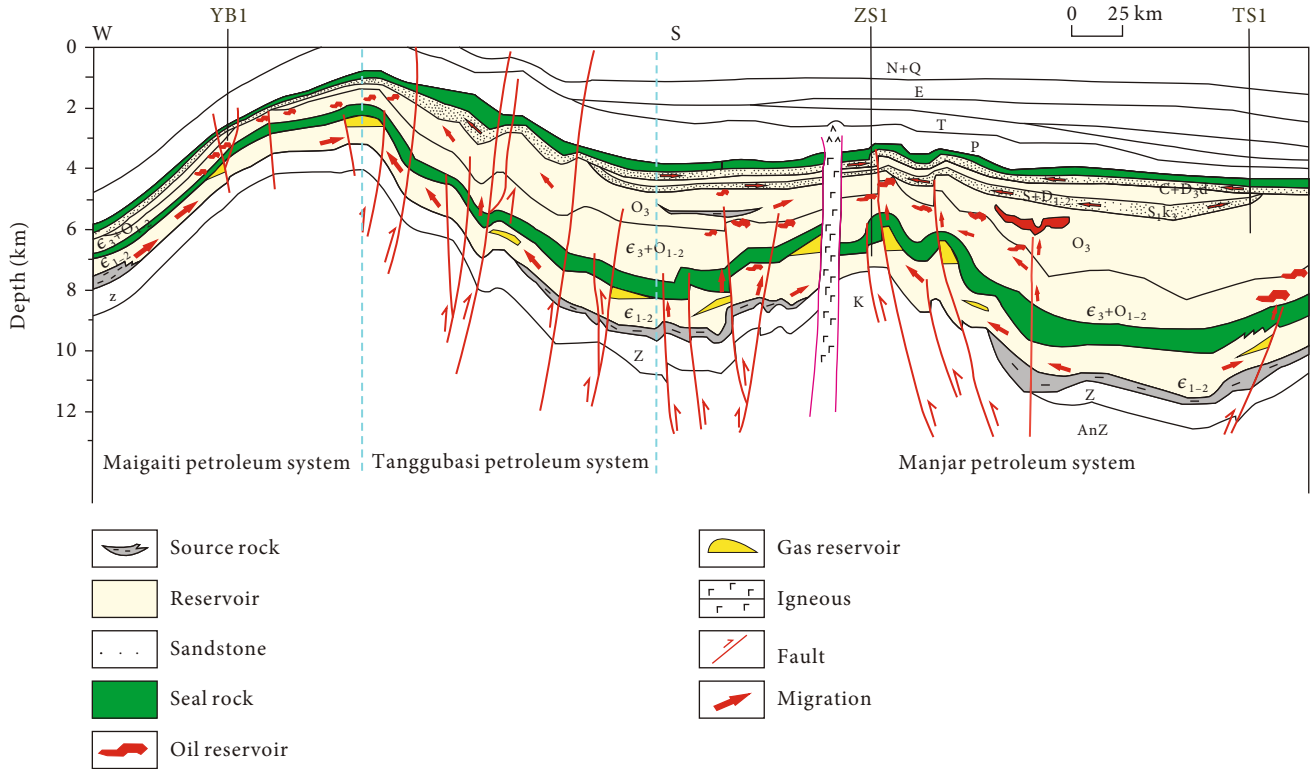

Figure 10: Profile of Cambrian petroleum system in the Tarim Basin.

the Tarim Basin, the Lower Cambrian petroleum system consists of the Lower Cambrian source rocks, the Xiaorbulak Formation, and the Middle Cambrian gypsolyte, and it is widely distributed in the basin. Based on the thermal evolution of the Lower Cambrian source rocks, the oil-gas migration and accumulation trends of the Xiaorbulak Formation were simulated during four critical phases (Figure 7).

It can be seen from the oil-gas migration processes of the petroleum system that the oil-gas charging began in the Middle Caledonian (Figure 7(a)), and the Hercynian was the liquid hydrocarbon accumulation period (Figures 7(b) and 7(c)). The gaseous hydrocarbons mainly accumulated in the Himalayan (Figure 7(d)). The hydrocarbon reservoir formation was characterized by early oil and late gas accumulation. According to the analysis of the four petroleum systems, the streamline was long in the Early Caledonian and Hercynian and was characterized by a distant source and long-distance migration. As the maturity of the source rocks increased, the streamline began to widen and shorten, and there was a distant source charging between the source and traps. The streamline accumulation occurred in the paleo uplifts. The Katake uplift is characterized by multisource charging accumulation due to the influence of the Manjar, Awati, and Tanggubasi petroleum systems and is the most favorable oil-gas accumulation zone in the lower petroleum system in the interplatform basin. Owing to the combined charging from the petroleum systems in the Maigaiti slope and Tanggubasi depression, the west Bachu uplift is a favorable oil-gas accumulation zone in the lower petroleum system. Owing to the continuous charging of the single petroleum system, the east Bachu uplift and the Tabei uplift are favorable oil-gas accumulation zones in the lower petroleum system. In addition, the area surrounding the dominant migration channel is also a favorable oil-gas accumulation zone. Based on the analysis of the oil-gas migration and accumulation trends in the Himalayan (Figure 7(d)), the Manjar petroleum system, Awati petroleum system, and Maigaiti slope petroleum system have developed 11, five, and eight dominant migration channels, respectively, which are favorable target areas for evaluating the gas reservoir in the lower petroleum system.

According to the oil-gas indications in the drilling wells throughout the entire basin, good oil-gas indications have been observed in the Xiaorbulak Formation in the Bachu and Tabei areas [49, 50]. Bitumen has been found in the Xiaorbulak Formation in well ST1 in east Bachu, and a gas production rate of $3.02 \times 104\ m^3/d$ has been obtained from the Xiaorbulak Formation in well ZS1. A high yield of light crude oil has been obtained from well LT 1 in the Xiaorbulak Formation in the northern part of the Tarim Basin [30]. In addition, good oil-gas indications have been observed in the lower petroleum system in wells TC1, K 2, and H 4, which demonstrates the large oil-gas accumulation potential of the Lower Cambrian Xiaorbulak Formation [51]. The results of the streamline modeling are consistent with the above oil-gas indications and the hydrocarbon generation and expulsion histories of the single wells, indicating that the oil-gas accumulation modeling has a good reference value.

4.4. Oil-Gas Accumulation in the Upper Petroleum System. The Upper Cambrian petroleum system consists of the

Lower Cambrian source rocks and the Lower Ordovician Lower Qiulitage Group and Penglaiba Formation, and it is widely distributed throughout the entire basin. In this study, the oil-gas charging process of the upper petroleum system was reconstructed using the streamline method, and it was found that the characteristics and trends of the streamline variations were consistent with those of the lower petroleum system (Figure 8). This indicates that the oil-gas charging, migration, and accumulation trends of the petroleum system have significant inheritance characteristics. It can be seen from Figure 8 that the uplift of the upper petroleum system and the dominant migration channel in the slope are positive zones for oil-gas accumulation. Unlike the lower petroleum system, the Manjar petroleum system is characterized by significant streamline accumulation in the Guchengxu uplift and the northern part of the Tarim Basin, and the oil-gas migration and accumulation trends increase significantly. This will be discussed further below.

Regarding the Lower Qiulitage Group, oil-gas indications have been observed in wells BT5 and MB1 in the Bachu area and well ZS1 in the middle of the Tarim Basin. Abnormal gas measurements have been obtained at 7158–7510 m in well YQ6 in the Lower Qiulitage Group in the northern part of the Tarim Basin, and oil patch and oil stains have been observed in well TS1 in the Lower Qiulitage Group [15]. All of these observations indicate a promising oil-gas potential. Based on the thermal evolution of the Lower Cambrian source rocks, the oil-gas migration and accumulation trends of the Lower Qiulitage Group in the Hercynian (Figure 8(a)) and Himalayan (Figure 8(b)) were reconstructed and modeled. The modeling results are consistent with the above oil-gas indications in the single wells and the hydrocarbon generation and expulsion histories of the single wells.

5. Discussion

The Cambrian oil-gas migration process in the Tarim Basin is an important basis for evaluating the deep oil-gas resources [17, 33, 52]. However, it is extremely difficult to study the migration in the Cambrian deep petroleum system in the Tarim Basin, and there are few reports on the regularity of the oil-gas accumulation due to the low degree of exploration [3]. Through thermal history reconstruction (Figure 3), our basin simulation revealed that the Cambrian source rocks in the Tarim Basin are mainly in the highly mature and overmature stages. The simulation of the hydrocarbon charging phases in the different geological periods (Figure 4) revealed that the oil generation in the source rocks predominantly occurred from the Caledonian to Hercynian, and the gas generation occurred from the Indosinian to Himalayan. The distribution range of the effective source rocks was determined from the planar thermal evolution of the source rocks (Figure 6), and the fluid potential distributions of the Upper and Lower Cambrian hydrocarbon systems were simulated based on the geomorphology provided by the paleotectonic evolution (Figures 7 and 8).

Based on the fluid potential modeling conducted in this study, the paleostructural characteristics of the petroleum system and the maturity of the source rocks were comprehensively considered to reconstruct the forms and characteristics of the streamline distribution during the critical time periods and to identify the four development models of the oil-gas charging and migration in the Cambrian (Figure 9). The four oil-gas charging models were significantly different. The first model was characterized by multisource, multiphase, and multidirectional accumulation (Figures 9(a) and 9(b)). Owing to the combined charging influences of the multiple petroleum systems, the oil and gas were charged from multiple directions toward the low-potential zone. Owing to the strong oil-gas charging intensity, the oil and gas existed in the phase state. It was mainly distributed in the Manjar, Awati, and Tanggubasi petroleum systems, and the oil-gas accumulation occurred in the Katake uplift and the Shuntuoguole low uplift. The second model was characterized by multisource, multiphase, and single-directional accumulation (Figures 9(c) and 9(d)). Owing to the combined charging influences of the multiple oil-gas petroleum systems, the oil and gas migrated in a single direction, from the depression (high fluid potential zone) to the uplift (low fluid potential zone). Owing to the large oil-gas charging intensity, an oil-gas reservoir was mainly formed. This was the typical model in the intersection zone of the Maigaiti and Tanggubasi petroleum systems, and the oil-gas accumulation occurred in the southwest Bachu uplift. The third model was characterized by single-source, multiphase, and multidirectional accumulation (Figures 9(e) and 9(f)). Under the control of a single petroleum system, the oil and gas migrated from the side and bottom into the low-potential zone. Owing to the influence of the differential displacement, a gas reservoir was mainly formed. This was the typical model in the Tabei uplift, and the oil-gas accumulation mainly occurred in the Manjar petroleum system. The fourth model was characterized by single-source, multiphase, and single-directional accumulation (Figures 9(g) and 9(h)). Owing to the influence of the single petroleum system, the oil and gas migrated along a single direction, from the high potential zone to the low-potential zone. In addition, a gas reservoir was mainly formed due to the differential displacement. This was the typical model in the petroleum system in the Bachu and Maigaiti slope, and the oil-gas accumulation mainly occurred in the southwest Bachu uplift.

Previous studies have chiefly analyzed the geological features and predicted that the uplift may be a favorable area for deep oil-gas accumulation based on the structural level and oil-gas indications [26, 53], but few studies have considered the oil-gas charging intensity and migration model, and therefore, they lack a basis for evaluating the favorable areas.

In this study, the hydrocarbon migration direction and path of the deep Cambrian oil and gas migration were determined from the perspective of the kinetic energy and potential energy of the fluid based on the source rock and paleogeomorphic factors. Our research results are consistent with the current exploration situation, indicating that the above research represents good progress. The analysis of the results of the basic fluid potential simulation revealed that the Katake uplift was the most favorable zone for

Cambrian oil-gas migration and accumulation, and it was a multisource and multiphase accumulation zone of the Manjar petroleum system, Awati petroleum system, and Tanggubasi petroleum system. As a result, the high oil-gas charging intensity and long charging time were beneficial to oil-gas entrapment in the Cambrian system. The Shuntuoguole low uplift was charged from the Manjar petroleum system and the Awati petroleum system and had an inferior oil-gas charging intensity (Figure 10). The southwest Bachu uplift was charged from the Maigaiti petroleum system and the Tanggubasi petroleum system, which was beneficial to Cambrian oil-gas accumulation. Owing to the long-term and continuous charging from the Manjar petroleum system, the Tabei uplift was also a favorable zone for Cambrian oil-gas accumulation. The comparison of the oil-gas migration and accumulation trends of the Upper and Lower Cambrian petroleum systems indicates a better consistency (Figure 10). It reflects the significant control of the paleostructural evolution on the ultradeep oil-gas accumulation in the Cambrian system, and it further reveals that the traps of the dominant migration channel of the oil-gas accumulation may be a promising target for the development of the ultradeep paleo oil-gas reservoir in the Cambrian system. The above results are consistent with the potential of the current oil-gas resources explored in the current shallow layer, reflecting the effectiveness and high application value of the proposed method.

6. Conclusions

The secondary migration of deep oil-gas system first identified the thermal evolution history and model of source rocks. The history of the hydrocarbon generation in the Lower Cambrian source rocks in the Tarim Basin was characterized by early oil generation and late gas generation, and three models occurred under the influence of the paleostructural evolution. The continuous thermal evolution model occurred in the depression, e.g., the hydrocarbons were generated in the Early Ordovician. The peak liquid hydrocarbon generation occurred from the Devonian to the Carboniferous, the peak gas generation occurred in the Early Permian, and the hydrocarbon generation was not interrupted. The continuous thermal evolution model occurred in the slope, i.e., the hydrocarbons were generated in the Upper Ordovician strata. The hydrocarbon expulsion occurred in the Carboniferous, the peak liquid hydrocarbon generation occurred in the Permian, and the peak gaseous hydrocarbon generation occurred in the Triassic. The hydrocarbon generation process occurred in stages. The fast thermal evolution model occurred in the mountain front in the peripheral basin. The degree of thermal evolution increased rapidly after the Miocene, and the oil generation and gas generation reached a peak. This was the late fast hydrocarbon generation model.

There are four models of the fluid potential developed in the Cambrian ultradeep reservoir in Tarim Basin, i.e., multisource, multiphase, multidirectional accumulation; multisource, multiphase, single-directional accumulation; single-source, multiphase, multidirectional accumulation; and single-source, multiphase, single-directional accumulation. The multisource, multiphase, multidirectional accumulation and the multisource, multiphase, single-directional accumulation were the most beneficial models for oil-gas accumulation due to the strong charging intensity and long charging time.

The migration trend in the Upper and Lower Cambrian petroleum systems in the Tarim Basin has significant inheritance characteristics. The streamline accumulation in the uplift and slope reflects the dominant migration channel, which is favorable for oil-gas accumulation. The Katake uplift and the southwest Bachu uplift experienced multisource charging accumulation and are the most favorable oil-gas accumulation zones in the Cambrian petroleum system. The east Bachu uplift and the Tabei uplift are more favorable oil-gas accumulation zones due to continuous charging of the single petroleum system.

The basin modeling technique can provide an effective reference for evaluation of the migration and accumulation in the Cambrian petroleum system in the Tarim Basin. The prerequisite is geological model data for the thermal evolution of the source rocks and the evolution of the top structure of the reservoir.

Data Availability

The data that support the finds of this study are available from the corresponding author upon reasonable request.

Conflicts of Interest

The authors declare that they have no known competing financial interests or personal relationships that could have appeared to influence the work reported in this paper.

Acknowledgments

This research was supported by the Regional Innovation Cooperation Project (grant number 21QYCX0048) of the Science and Technology Department of Sichuan Province. We are grateful to the SINOPEC Northwest Company and the Research Institute of Petroleum Exploration & Development for providing some important data.

References

[1] J. Q. Chen, K. Ma, X. Pang, and H. Yang, "Secondary migration of hydrocarbons in Ordovician carbonate reservoirs in the Lunnan area, Tarim Basin," *Journal of Petroleum Science and Engineering*, vol. 188, article 106962, 2020.

[2] J. Song, T. Chen, and J. Zhang, "Permian and Triassic hydrocarbon migration and accumulation in the Cainan area, Junggar Basin, China," *Journal of Petroleum Science and Engineering*, vol. 210, article 109965, 2022.

[3] R. K. Bian, J. C. Zhang, X. Tang, L. Yun, and S. L. Jiang, "Characteristics of energy fields and the hydrocarbon migration-accumulation in deep strata of Tahe oilfield, Tarim Basin, NW China," *Petroleum Exploration and Development Online*, vol. 37, no. 4, pp. 416–423, 2010.

[4] A. Zhurvaljov, Z. Lanetc, N. Khoperskaya, and S. S. Rahman, "A simple approach to increasing computational efficiency of numerical simulations of hydrocarbon migration based on the Darcy flow concept," *Computers & Geosciences*, vol. 157, article 104915, 2021.

[5] G. A. Osukuku, O. O. Osinowo, and C. Orora, "Integrated fluid inclusion studies and source rock parameters in constraining hydrocarbon potential in offshore Lamu Basin, Kenya," *Energy Geoscience*, vol. 4, no. 3, article 100142, 2023.

[6] D. J. Byrne, P. H. Barry, and C. J. Ballentine, "The use of noble gas isotopes to constrain subsurface fluid flow and hydrocarbon migration in the East Texas Basin," *Geochimica et Cosmochimica Acta*, vol. 268, pp. 186–208, 2020.

[7] G. Chi, D. Lavoie, R. Bertrand, and M.-K. Lee, "Potential hydrocarbon migration paths predicted from numerical modeling of basinal fluid flow in the Paleozoic Anticosti Basin, eastern Canada," *Journal of Geochemical Exploration*, vol. 101, no. 1, p. 26, 2009.

[8] P. Elena, H. Christian, and H. Matthias, "3-D numerical modelling of methane hydrate accumulations using PetroMod," *Marine and Petroleum Geology*, vol. 71, pp. 288–295, 2016.

[9] E. A. Abd El Gawad, M. F. Ghanem, M. M. Lotfy, D. A. Mousa, M. G. Temraz, and A. M. Shehata, "Burial and thermal history simulation of the subsurface Paleozoic source rocks in Faghur basin, North Western Desert, Egypt: implication for hydrocarbon generation and expulsion history," *Egyptian Journal of Petroleum*, vol. 28, pp. 261–271, 2019.

[10] J. Bourdet, R. H. Kempton, V. Dyja-Person, J. Pironon, S. Gong, and A. S. Ross, "Constraining the timing and evolution of hydrocarbon migration in the Bight Basin," *Marine and Petroleum Geology*, vol. 114, article 104193, 2020.

[11] H. Qu, B. Yang, S. Gao et al., "Controls on hydrocarbon accumulation by facies and fluid potential in large- scale lacustrine petroliferous basins in compressional settings: a case study of the Mesozoic Ordos Basin, China," *Marine and Petroleum Geology*, vol. 122, article 104668, 2020.

[12] Y. M. Makeen, W. H. Abdullah, M. J. Pearson et al., "History of hydrocarbon generation, migration and accumulation in the Fula sub- basin, Muglad Basin, Sudan: implications of a 2D basin modeling study," *Marine and Petroleum Geology*, vol. 77, pp. 931–941, 2016.

[13] J. X. Chen, X. W. Guo, Y. J. Han, and S. He, "Combination of basin modelling and carbazoles to investigate secondary oil migration pathways in the Dongying depression of the Bohai Bay Basin, China," *Marine and Petroleum Geology*, vol. 131, article 105163, 2021.

[14] T. Tian, P. Yang, Z. Ren et al., "Hydrocarbon migration and accumulation in the lower Cambrian to Neoproterozoic reservoirs in the Micangshan tectonic zone, China: new evidence of fluid inclusions," *Energy Reports*, vol. 6, pp. 721–733, 2020.

[15] Z. M. Wang, H. W. Xie, Y. Q. Chen, Y. M. Qi, and K. Zhang, "The discovery and exploration significance of Cambrian subsalt primary Baiyun reservoir in Zhongshen no. 1 well in Tarim Basin," *China Petroleum Exploration*, vol. 19, pp. 1–13, 2014.

[16] F. Z. Jiao, "Significance of oil and gas exploration in the strike-slip fault zone in Shuntogol area, Tarim Basin," *Oil & Gas Geology*, vol. 38, pp. 831–839, 2017.

[17] W. E. Guoqi, Z. H. Yongjin, J. Zheng et al., "Tectonic-lithofacies paleogeography, large-scale source-reservoir distribution and exploration zones of Cambrian subsalt formation, Tarim Basin, NW China," *Petroleum Exploration and Development*, vol. 48, pp. 1289–1303, 2021.

[18] Y. Gu, Y. L. Wan, J. W. Huang, X. J. Zhuang, B. Wang, and M. Li, "Prospect of ultra-deep oil and gas exploration in the Tarim Basin under the condition of "large burial depth and high pressure"," *Petroleum Experimental Geology*, vol. 41, pp. 157–164, 2019.

[19] J. C. Zheng, B. Ll, H. Y. Wu, and Q. Yuan, "Study on thermal evolution history and hydrocarbon relationship of source rocks based on basin simulation technology – a case study of the Yultus Formation in Tarim Basin," *Petroleum Geology and Recovery*, vol. 25, pp. 39–49, 2018.

[20] H. J. Yang, Y. Q. Chen, J. Tian, and J. H. Du, "Major discoveries and significance of oil and gas exploration in the ultra-deep strata of well 1 in the roundtable exploration of the Tarim Basin," *China Petroleum Exploration*, vol. 25, pp. 62–72, 2020.

[21] M. Zhao, Z. Wang, W. Pan, and S. Liu, "Lower Palaeozoic source rocks in Manjiaer sag, Tarim Basin," *Petroleum Exploration and Development*, vol. 35, no. 4, pp. 417–423, 2008.

[22] N. S. Qiu, J. Chang, Y. H. Zuo, J. Y. Wang, and H. L. Li, "Thermal evolution and maturation of lower Paleozoic source rocks in the Tarim Basin, Northwest China," *AAPG Bulletin*, vol. 96, no. 5, pp. 789–821, 2012.

[23] Z. Huo, X. Pang, X. Ouyang et al., "Upper limit of maturity for hydrocarbon generation in carbonate source rocks in the Tarim Basin platform, China," *Arabian Journal of Geosciences*, vol. 8, no. 5, pp. 2497–2514, 2015.

[24] C. Lin, H. Li, and J. Liu, "Major unconformities, tectonostratigraphic frameword, and evolution of the superimposed Tarim Basin, Northwest China," *Journal of Earth Science*, vol. 23, no. 4, pp. 395–407, 2012.

[25] S. Wang, M. Zheng, X. Liu, X. Niu, W. Chen, and K. Su, "Distribution of Cambrian salt-bearing basins in China and its significance for halite and potash finding," *Journal of Earth Science*, vol. 24, no. 2, pp. 212–233, 2013.

[26] J. Du and W. Pan, "Accumulation conditions and play targets of oil and gas in the Cambrian subsalt dolomite, Tarim Basin, NW China," *Petroleum Exploration and Development*, vol. 43, no. 3, pp. 360–374, 2016.

[27] R. Zhao, Y. Liang, J. Zhao, H. Yang, and Y. Wu, "Division and correlation of the upper-middle Cambrian evaporate platform facies dolomite formation in Tarim Basin," *Geochemistry International*, vol. 57, no. 2, pp. 206–226, 2019.

[28] Y. Zhang, D. Chen, X. Zhou, Z. Guo, W. Wei, and M. Mutti, "Depositional facies and stratal cyclicity of dolomites un the lower Qiulitag group (upper Cambrian) in northwestern Tarim Basin, NW China," *Facies*, vol. 61, no. 1, pp. 1–24, 2015.

[29] G. Y. Zhu, F. R. Chen, Z. Y. Chen et al., "Discovery and basic characteristics of high-quality source rocks found in the Yuertusi Formation of the Cambrian in Tarim Basin, China," *Natural Gas Geoscience*, vol. 1, no. 1, pp. 21–33, 2016.

[30] P. Yang, G. Wu, Z. Ren, R. Zhou, J. Zhao, and L. Zhang, "Tectono-thermal evolution of Cambrian-Ordovician source rocks and implications for hydrocarbon generation in the eastern Tarim Basin, NW China," *Journal of Asian Earth Sciences*, vol. 194, article 104267, 2020.

[31] L. Wu, G. Zhu, L. Yan, X. Feng, and Z. Zhang, "Late Ediacaran to early Cambrian tectonic-sedimentary controls on lower Cambrian black shales in the Tarim Basin, Northwest China, Northwest China," *Global and Planetary Change*, vol. 205, article 103612, 2021.

[32] A. J. Shen, J. F. Zheng, Y. Q. Chen, X. F. Ni, and L. L. Huang, "Characteristics, origin and distribution of dolomite reservoirs in lower- middle Cambrian, Tarim Basin, NW China," *Petroleum Exploration and Development*, vol. 43, no. 3, pp. 375–385, 2016.

[33] G. Zhu, T. Li, Z. Zhang et al., "Distribution and geodynamic setting of the late Neoproterozoic– early Cambrian hydrocarbon source rocks in the South China and Tarim Blocks," *Journal of Asian Earth Sciences*, vol. 201, article 104504, 2020.

[34] M. P. Li, Z. Chen, S. Yi et al., "Origin and accumulation mechanisms of deep paleozoic oil and gas: a case study of the Central Tarim basin, western China," *Journal of Petroleum Science and Engineering*, vol. 208, article 109634, 2022.

[35] S. W. Guan, C. Zhang, R. Ren et al., "Early Cambrian syndepositional structure of the northern Tarim Basin and a discussion of Cambrian subsalt and deep exploration," *Petroleum Exploration and Development*, vol. 46, no. 6, pp. 1141–1152, 2019.

[36] A. Schito, S. Corrado, L. Aldega, and D. Grido, "Overcoming pitfalls of vitrinite reflectance measurements in the assessment of thermal maturity: the case history of the lower Congo basin," *Marine and Petroleum Geology*, vol. 74, pp. 59–70, 2016.

[37] S. Jiang, Y. Zuo, M. Yang, and R. Feng, "Reconstruction of the Cenozoic tectono-thermal history of the Dongpu depression, Bohai Bay basin, China: constraints from apatite fission track and vitrinite reflectance data," *Journal of Petroleum Science and Engineering*, vol. 205, article 108809, 2021.

[38] C. Lin, H. Li, and J. Liu, "Major unconformities, tectonostratigraphic framework, and evolution of the superimposed Tarim Basin, Northwest China," *Journal of Earth Science*, vol. 23, pp. 395–407, 2012.

[39] N. Van Su, N. Van Kieu, B. V. Dung, and T. D. Cuong, "Biostratigraphy and palaeoenvironments of early Pleistocene deposits in the southern part of the Gulf of Tonkin, Vietnam," *Quaternary International*, vol. 604, pp. 1–15, 2021.

[40] Z. L. Ren, T. Tian, J. S. Li, and J. P. Wang, "Research methods of thermal evolution history of sedimentary basins and research progress of thermal evolution history restoration of superposition basins," *Journal of Earth Sciences and Environment*, vol. 36, pp. 430–438, 2014.

[41] B. Ni, L. J. Tang, M. Li, and Z. H. Song, "Structural characteristics, formation mechanism and hydrocarbon geological significance of Niaoshan fault zone in Tarim Basin," *Natural Gas Geoscience*, vol. 29, pp. 834–844, 2018.

[42] D. Y. Wang, Y. P. Cheng, L. Wang, and H. X. Zhou, "Controlling factors of coalbed methane occurrence below redbeds in Xutuan mine: caprock thickness below redbeds," *Journal of Natural Gas Science and Engineering*, vol. 96, article 104323, 2021.

[43] J. R. Allwardt, G. E. Michael, C. R. Shearer, P. D. Heppard, and H. Ge, "2D modeling of overpressure in a salt withdrawal basin, Gulf of Mexico, USA," *Marine and Petroleum Geology*, vol. 26, no. 4, pp. 464–473, 2009.

[44] D. F. Qiu, S. J. Li, Y. S. Yuan, X. P. Mao, Y. Zhou, and D. S. Sun, "Geohistory modeling and its petroleum geological significance of middle-upper Yangtze area," *Petroleum Geology and Recovery Efficiency*, vol. 22, pp. 6–14, 2015.

[45] Z. Jiang, Y. Li, H. Du, and Y. Zhang, "The Cenozoic structural evolution and its influences on gas accumulation in the Lishui sag, East China Sea Shelf Basin," *Journal of Natural Gas Science and Engineering*, vol. 22, pp. 107–118, 2015.

[46] M. Nuzzo, Y. Tomonaga, M. Schmidt, and V. Valadares, "Formation and migration of hydrocarbons in deeply buried sediments of the Gulf of Cadiz convergent plate boundary - insights from the hydrocarbon and helium isotope geochemistry of mud volcano fluids," *Marine Geology*, vol. 410, pp. 56–69, 2019.

[47] J. Wan, Y. Gong, W. Huang, Q. Zhuo, and X. Lu, "Characteristics of hydrocarbon migration and accumulation in the lower Jurassic reservoirs in the Tugerming area of the eastern Kuqa depression, Tarim Basin," *Journal of Petroleum Science and Engineering*, vol. 208, article 109748, 2022.

[48] P. Yang, K. Y. Liu, J. L. Liu et al., "Petroleum charge history of deeply buried carbonate reservoirs in the Shuntuoguole low uplift, Tarim Basin, West China," *Marine and Petroleum Geology*, vol. 128, article 105063, 2021.

[49] D. W. Wang, T. G. Wang, M. J. Li, and D. G. Song, "Alkyl distribution characteristics and oil source implications of Wells no. 5 and no. 1 in the tower uplift," *Geochemical*, vol. 45, pp. 451–461, 2016.

[50] D. F. Song, T. G. Wang, and M. J. Ll, "Geochemical characteristics of hydrocarbons in the Cambrian system under salt in Wells Zhongshen 1 and Zhongshen 1C in the Tazhong area," *Science China Earth Sciences*, vol. 46, pp. 107–117, 2016.

[51] M. Y. Hu, C. Y. Sun, and D. Gao, "Characteristics of tectonic-lithofacies paleogeography in the lower Cambrian Xiaoerbulake formation, Tarim Basin," *Oil & Gas Geology*, vol. 40, pp. 12–23, 2019.

[52] X. Zhou, X. Lu, G. Zhu, Y. Cao, L. Yan, and Z. J. Zhang, "Origin and formation of deep and superdeep strata gas from Gucheng-Shunnan block of the Tarim Basin, NW China," *Journal of Petroleum Science and Engineering*, vol. 177, pp. 361–373, 2019.

[53] B. Zhou, H. L. Li, J. B. Yun, Z. M. Xu, and F. Feng, "Petroleum accumulation system evaluation of carbonate oil and gas: a case study of Cambrian in Tarim Basin," *Petroleum Geology & Experiment*, vol. 42, pp. 132–138, 2020.